ResearchGate

See discussions, stats, and author profiles for this publication at: https://www.researchgate.net/publication/342064601

Influence of interfacial magnetic ordering and field-cooling effect on perpendicular exchange bias and magnetoresistance in nanoporous IrMn/[Co/Pd] films

Article *in* Journal of Applied Physics · June 2020

DOI: 10.1063/5.0006194

CITATION
1

READS
101

14 authors, including:

J. Kasiuk
Belarusian State University
36 PUBLICATIONS **293** CITATIONS
SEE PROFILE

Anh T.N. Nguyen
Vietnam Academy of Science and Technology
35 PUBLICATIONS **664** CITATIONS
SEE PROFILE

J. Fedotova
Belarusian State University
123 PUBLICATIONS **857** CITATIONS
SEE PROFILE

Olga Kupreeva
Belarusian State University of Informatics and Radioelectronics
20 PUBLICATIONS **68** CITATIONS
SEE PROFILE

Some of the authors of this publication are also working on these related projects:

NAFOSTED 103.03.2015-85 View project

The Science and Technology Project of Vietnam Academy of Science and Technology View project

All content following this page was uploaded by Lazarouk Serguei on 15 June 2020.

The user has requested enhancement of the downloaded file.

ACCEPTED MANUSCRIPT

Journal of Applied Physics

AIP Publishing

This is the author's peer reviewed, accepted manuscript. However, the online version of record will be different from this version once it has been copyedited and typeset.
PLEASE CITE THIS ARTICLE AS DOI: 10.1063/5.0006194

Influence of interfacial magnetic ordering and field-cooling effect on perpendicular exchange bias and magnetoresistance in nanoporous IrMn/[Co/Pd] films

Wen-Bin Wu[1], Julia Kasiuk[1*], Thi Ngoc Anh Nguyen[2,3], Janusz Przewoźnik[4], Julia Fedotova[1], Czeslaw Kapusta[4], Olga Kupreeva[5], Serguei Lazarouk[5], Khanh Tung Do[2], Thanh Huong Nguyen[2], Hong Ky Vu[2], Pham Hoai Linh[2], Lam D. Vu[2,3], Johan Åkerman[6]

[1]Institute for Nuclear Problems, Belarusian State University, Minsk 220006, Belarus
[2]Institute of Materials Science, Vietnam Academy of Science and Technology, 18 Hoang Quoc Viet, Cau Giay, Hanoi 11355, Vietnam
[3]Graduate University of Science and Technology, Vietnam Academy of Science and Technology, 18 Hoang Quoc Viet, Cau Giay, Hanoi 11355, Vietnam
[4]AGH University of Science and Technology, Faculty of Physics and Applied Computer Science, Department of Solid State Physics, Krakow 30-059, Poland
[5]Belarusian State University of Informatics and Radioelectronics, Minsk 220013, Belarus
[6]Department of Physics, University of Gothenburg, Göteborg 41296, Sweden

*corresponding author, julia-nechaj@yandex.ru

We have studied systematically the effect of field cooling on the magnetic properties of continuous and porous IrMn/[Co/Pd] films. It is found that the coexistence of two ferromagnetic (FM) phases in the porous film, namely, hard-magnetic and soft-magnetic ones, with significantly different magnetic properties relates to the role of pore edges and modifies its magnetic and magnetoresistive properties. It is shown that annealing of the films with their subsequent cooling in an external magnetic field applied for aligning the magnetic moments in the antiferromagnetic (AFM) IrMn layer improves effectively the uniaxial perpendicular anisotropy of the [Co/Pd] layer and induces unidirectional anisotropy in its hard-magnetic regions, blocking simultaneously the soft-magnetic parts by pinning their magnetic moments along the film plane. Magnetoresistance of both continuous and porous films is found to be determined mainly by electron-magnon scattering, whereas the complex morphology of the porous film providing different orientation of exchange coupling at the AFM/FM interface in different film's regions modifies significantly spin-dependent electron transport. The revealed asymmetry of the field dependences of magnetoresistance is attributed both to unidirectional magnetic anisotropy of the FM layer and its splitting into magnetically nonequivalent regions in the porous films. The origin of the observed phenomenon is associated with a local influence on the orientation of AFM magnetic moments by an adjacent ferromagnet.

ACCEPTED MANUSCRIPT
Journal of Applied Physics
AIP Publishing
This is the author's peer reviewed, accepted manuscript. However, the online version of record will be different from this version once it has been copyedited and typeset.
PLEASE CITE THIS ARTICLE AS DOI: 10.1063/5.0006194

I. INTRODUCTION

It is well known that a ferromagnetic (FM) layer in contact with an antiferromagnetic (AFM) material demonstrates unidirectional exchange anisotropy[1] appearing commonly as a shift of magnetization hysteresis loop after cooling the system through Néel temperature T_N of the AFM layer in an external magnetic field. Exchange bias (EB) originating from the exchange coupling between AFM and FM magnetic moments at their AFM/FM interface is one of the basic phenomena determining the application of the related structures in spintronics, for exploiting them in read heads[2], sensors[3] and magnetic random access memory[4]. For tuning the desirable properties of AFM/FM systems aimed at corresponding application tasks, deep understanding of the physical principles which rules their parameters is required. Regarding exchange-bias related effects, although the phenomenon of AFM/FM coupling has been studied for more than half a century starting from 1956[5], the underlying physical theory explaining it exhaustively is still under discussion. The main questions concerning the ordering of interfacial spins need to be clarified. The matter is that the model developed by Meiklejohn and Bean[5] is revealed to overestimate significantly the magnitude of the exchange bias field H_E[6]. Additionally, it cannot describe the simultaneous occurrence of nonzero H_E and increased H_C parameters observed in many AFM/FM exchange-coupled systems[6]. Numerous models were proposed to correct its limitations which analyzed domain walls inside the AFM layer parallel to the AFM/FM interface[6,7], a random exchange interaction due to atomic-scale interface roughness[8], uncompensated interfacial AFM spins[1,9], etc. Despite different approaches, the main point for understanding field-dependent behavior of AFM/FM bilayers is to determine spins arrangement in the AFM layer, particularly, in the near-interface regions, since only a part of the AFM layer that is in contact with the FM layer is involved in the EB coupling due to a short-range character of the FM-AFM exchange interaction[10]. Unfortunately, only a few experimental methods allow their "direct" visualizing, namely neutron diffraction and X-ray magnetic dichroism spectroscopy[11] which require complex, costly and rare equipment. Taking into account the poor availability of these experimental facilities and difficult results interpretation needed, indirect methods of study based on the influence of AFM coupled layer on the basic properties of the AFM/FM systems have found broad application. Particularly, the methods exploiting an anisotropic magnetoresistance (MR) effect[12] are widely used.

It should be additionally emphasized, that the majority of the numerous studies on the exchange bias phenomenon have been carried out for the films with in-plane magnetic anisotropy[6-9,12]. The conducted researches produced the developed theory describing the bias-related phenomena in these

ACCEPTED MANUSCRIPT
Journal of Applied Physics
AIP Publishing
This is the author's peer reviewed, accepted manuscript. However, the online version of record will be different from this version once it has been copyedited and typeset.
PLEASE CITE THIS ARTICLE AS DOI: 10.1063/5.0006194

systems[13,14]. A more complex origin of exchange bias coupling in the multilayers (MLs) with perpendicular magnetic anisotropy (PMA) results in a more discrepant explanation of the observed phenomena[4,10,15-18] that is accompanied by less numerous studies of such materials, and provides the necessity of elaborating the consistent theory describing the perpendicular exchange bias (PEB) and the mechanisms of the related effects arising.

The difficulty in interpreting the EB phenomenon lies in a complex mutual influence of FM and AFM layers. In this case, their relative position plays an important role in the observed effects. Unlike the commonly studied films stacks with an AFM layer grown on top of an anisotropic FM layer, where the former undergoes a strong ordering influence of the latter during deposition[19], the MLs with an AFM bottom layer demonstrate a more complex and rich spectrum of properties. Because of the almost "free" conditions of its ordering, the intrinsic properties of the bottom AFM layer should be considered for analyzing the observed effects, since they can interplay specifically with the magnetic structure of the adjacent FM layer. On the other hand, since there is no an ordering influence of the anisotropy field H_A of the pre-deposited FM layer, an additional cooling of the MLs with the bottom AFM layer in a magnetic field through T_N of the AFM layer is needed for the obtaining pronounced and stable PEB effect similar to that formed in the films with the top AFM layer just after deposition. Despite the "free" deposition conditions, it has been demonstrated, however, that the AFM spin structure is drastically altered after the FM layer has been deposited[10,20]. Understanding the difference between the effects that are induced by an external field H during field cooling (FC) and which appear spontaneously at the AFM/FM interface due to the anisotropies of both layers is the key point for describing interfacial spin ordering and interpretation of the mechanisms of evolution of spins configurations with changing external parameters (*T, H, time*). Moreover, a multifunctional role of AFM layer should be taken into account because it is not limited only by a passive pinning of the FM layer but also includes the active functions, such as an electrode in tunneling anisotropy MR, spin injector in devices based on the spin-Hall effect, etc.[21,22]

Due to the high Néel temperature, good corrosion resistance and high interface exchange energy[4,23,24], IrMn is a widely used AFM material in the exchange-biased systems. As it is previously determined, Néel temperature (T_N) of bulk phase of disordered γ-$IrMn_3$ equals to 730 K[25], but the exchange bias shift in the FM/AFM systems disappears at temperature higher than so called blocking temperature (T_B), which is typically lower than T_N of bulk AFM due to the finite-size and interfacial effects[26]. In 2002, M. Tsunoda, et al.[27] found that T_B of Co–Fe/Mn–Ir bilayers with the in-plane

ACCEPTED MANUSCRIPT
Journal of Applied Physics
AIP Publishing
This is the author's peer reviewed, accepted manuscript. However, the online version of record will be different from this version once it has been copyedited and typeset.
PLEASE CITE THIS ARTICLE AS DOI: 10.1063/5.0006194

unidirectional anisotropy depends on the thickness t of the AFM layer, changing from 493 K for t_{IrMn} = 5 nm to 563 K for t_{IrMn} = 10 nm. In 2005, J. Sort et al.[28] obtained [Pt/Co]/$IrMn_{5\ nm}$ system with PMA demonstrating $T_B \sim 400$ K and $H_E \sim 90$ Oe at $T = 300$ K after the film cooling in the field perpendicular to the film plane. Besides high T_B parameter essential for the use of exchange-biased bilayers in spintronic devices, their high M_r/M_S ratio (M_r defines the remanent magnetization, M_S is the saturation magnetization) and the coercive field (H_C) are also required. For satisfying the above demands and simultaneous implementation of the films splitting into low-size elements appropriate for high-density data storage and high-resolution magnetic sensing applications, their organizing in the form of nanodots[29] and antidot arrays[30,31] is generally accepted that allows obtaining nanoscale systems with the suitable magnetic parameters. High sensitivity of the films' magnetic properties to the size of elements, i.e. to the scale of the performed patterning reveals a strong necessity of their complex study in correlation with structural parameters of the patterned systems[31,32]. The formation of the antidot array is realized in the current study by means of the deposition of the AFM/FM MLs onto a porous substrate (template) containing small, nanoscale pores rather uniformly distributed over its surface. The pores serving as the domain-walls pinning sites confine[31] the nanosized regions of the magnetic films which are exchange-coupled with each other, but simultaneously demonstrate the features of separate nanostructures, such as rotational mechanisms of magnetization reversal[19,30]. In the frame of the concept of perpendicular percolated media[30-32], the implemented such a way nanopatterning is of practical interest for the mentioned applications, demonstrating the advantages of low-cost production, large-area covering and potential overcoming of the superparamagnetic limit due to the preserved coupling between the magnetic elements. Being able to influence the arrangement of magnetic moments in the film and interlayer magnetic interaction[19], the induced antidot (pores) array enriches the spectrum of detected magnetic and magnetoresistive properties of the film related to the complex effects at the pore edges and AFM/FM interface.

In this paper, the magnetic and magnetoresistive properties are compared for the continuous and porous IrMn/[Co/Pd] films obtained by deposition under the same conditions onto a flat Si/SiO_2 wafer and porous TiO_2 template, respectively, for elucidating the role of the porous morphology of the films. The main feature of the chosen composition is in the AFM *bottom* layer that allows to study the systems both with non-predetermined magnetic ordering/disordering of the IrMn layer after deposition and with the induced magnetic ordering in the IrMn layer in the direction defined by an external field during FC procedure. Considerable changes in the magnetization reversal of the porous films detected

ACCEPTED MANUSCRIPT
Journal of Applied Physics
AIP Publishing
This is the author's peer reviewed, accepted manuscript. However, the online version of record will be different from this version once it has been copyedited and typeset.
PLEASE CITE THIS ARTICLE AS DOI: 10.1063/5.0006194

after the AFM layer ordering are discussed in the context of non-uniform magnetic properties of the FM layer provided by its porosity.

II. EXPERIMENT

The procedure of obtaining the samples of the continuous and porous IrMn/[Co/Pd] films includes the following main steps. First, preparation of the porous templates of anodized titania on Si/SiO_2 wafers was carried out in accordance with the described previously procedure[33]. Briefly, 0.3 μm thick Ti film deposited on the silicon wafer is anodized in the solution containing 0.3% ammonium fluoride in ethylene glycol with 2 vol.% of water at low temperature of electrolyte. The anodization voltage was linearly increased from zero to 45–60 V at a rate of 1 V/s and then kept constant for the total anodization time, which was no longer than 35 min. The end of the anodization process was monitored by the drop of the anodic current density below 30% of its maximal value. Subsequent ion-plasma etching (Ar) during 100 min was applied for additional flattening of the surface relief of the templates. The templates will be denoted briefly from here as Si/TiO_2 templates.

Second, thin multilayered film with nominal composition of $Ta_{5nm}/Pd_{3nm}/IrMn_{6nm}/CoFe_{0.8nm}/[Co_{0.5nm}/Pd_{1nm}]_{\times 5}/Pd_{3nm}/Ta_{5nm}$ (briefly marked as IrMn/[Co/Pd]) was deposited both on the prepared porous Si/TiO_2 templates and flat Si/SiO_2 wafers under the same conditions in common experimental procedure by ultra-high vacuum magnetron sputtering in a 10^{-7} Pa high vacuum chamber (AJA International, Inc., USA). The Ta/Pd and Pd/Ta bilayers were applied as seed and capping layers for promoting the (111) texture and for preventing the oxidation of the multilayers, respectively[34,35]. The insertion of 0.8 nm CoFe layer between antiferromagnetic (IrMn) and ferromagnetic (Co/Pd) layers was used to enhance the exchange bias field (H_E), with the PMA of the entire system being almost unchanged[34]. The layer thicknesses were determined from the deposition time and the calibrated deposition rates. The deposition of the MLs was performed at room temperature (RT).

Then, for inducing unidirectional magnetic anisotropy, a portion of the samples was annealed at T_a = 500 K, namely they were heated up to T = 500 K (definitely above T_N), then placed in an external magnetic field of 5 kOe oriented normally to the films' plane and cooled in this field down to RT (hereafter this group of the samples will be marked as *annealed* films). Next, low-temperature magnetic and magnetoresistive parameters of the films, which were not preliminary annealed (they are defined as *as-deposited* films), were measured after zero-field cooling (ZFC) down to a

ACCEPTED MANUSCRIPT
Journal of Applied Physics
AIP Publishing
This is the author's peer reviewed, accepted manuscript. However, the online version of record will be different from this version once it has been copyedited and typeset.
PLEASE CITE THIS ARTICLE AS DOI: 10.1063/5.0006194

measurement temperature. On the contrary, the annealed films were cooled down to a measurement temperature in an external field (H_{FC} = 5 kOe) similar to that applied during the field cooling (FC) procedure after annealing. Summarizing, a schematic classification of the studied samples is shown in Fig. 1. Since a comprehensive study of the films was carried out some time after their deposition (excepting the initial characterization), the corresponding samples subjected to the detailed analysis are named as *relaxed* ones.

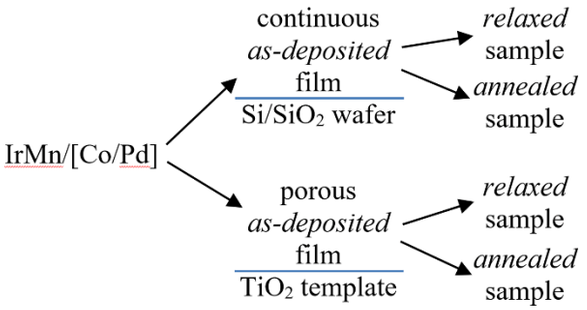

Fig. 1. Schematic classification of the studied samples of IrMn/[Co/Pd] film deposited onto two types of substrates (Si/SiO_2 wafer and Si/TiO_2 template) and partly annealed in a magnetic field of 5 kOe.

Surface morphology characterization of the porous Si/TiO_2 templates and the porous IrMn/[Co/Pd] films deposited over them was performed by scanning electron microscopy (SEM, HITACHI S-4800) at a voltage of 15 kV and Atomic Force Microscopy (AFM, NT-MDT Solver-Pro 47) using an NSG01 DLC supersharp diamondlike carbon tip with a curvature radius below 3 nm. The structure and phase composition of the continuous and porous films was examined by X-ray diffraction (XRD) using an Empyrean PANalytical diffractometer with Cu K_α radiation. The experimental data were collected at RT in two modes, namely, in the conventional Bragg-Brentano theta-theta geometry, with an angle 2theta (2θ) between the incident beam and detector being scanned in the range of 10-130 degrees, and in the grazing angle geometry at a fixed incidence angle of 5 degrees with respect to the samples' surfaces, with the detector scanning the 2θ space from 10 to 120 degrees. The latter geometry was used particularly for the analysis of phase composition of the porous films to avoid substantial overlapping the peaks from the film and template. The experimental data were analyzed with HighScore Plus software and fitted with the FullProf program[36] based on the Rietveld method. The magnetic properties of the continuous and porous IrMn-Co/Pd films were characterized using the vibrating sample magnetometry (VSM) option of the *Quantum Design* Physical Property Measurement System (PPMS) with an external magnetic field *H* up to 90 kOe applied along the film

ACCEPTED MANUSCRIPT
Journal of Applied Physics
AIP Publishing
This is the author's peer reviewed, accepted manuscript. However, the online version of record will be different from this version once it has been copyedited and typeset.
PLEASE CITE THIS ARTICLE AS DOI: 10.1063/5.0006194

normal and in the film plane direction in the temperature T range of 10-300 K. The linear contributions of diamagnetic signal from the films' substrates were subtracted from the experimental field dependences of magnetization $M(H)$. Measurements of the field dependences of electric resistance $R(H)$ were carried out using the resistivity option of the PPMS at T = 4-300 K. A linear press four-contact assembly was used for resistance R measurement using a square-wave excitation current with a frequency of 8.3 Hz applied along the films' surfaces both for the continuous and porous IrMn/[Co/Pd] films. A magnetic field up to 90 kOe was applied along the film normal. The corresponding field dependences of magnetoresistance (MR) were derived as $\Delta R(H)/R_0 = (R(H)-R_0)/R_0$, where $R_0 = R(0)$ is the resistance in zero external field.

III. RESULTS AND DISCUSSION

A. Structure and phase composition

Top-view SEM image of the as-deposited porous IrMn/[Co/Pd] film is shown in Fig. 2a. As it can be seen from the figure, the morphology of the film sputtered over Si/TiO_2 template is determined by pores array initiated by the template surface relief[19]. The mean diameter of pores at the film's surface is about 20 nm and is smaller than that for the template used (~30 nm[19]) indicating conic shape of the pores inside the film. The mean distance between the pores is about 150 nm, with the circular areas being formed between pores, which are well-detected in planar SEM image (Fig. 2a). A lighter color of these areas indicates their prominent roughness which is formed due to the developed surface relief of the porous template used. The developed surface relief of the porous film with the prominent hemispherical convexities is confirmed by AFM (Fig. 2b, d). The amplitude of the relief fluctuations (height of the convexities) is estimated to be 30-40 nm, with their planar size being close to the interpore distance. The average surface roughness ΔR, which is found to be ~11 nm, exceeds significantly the corresponding parameter of the continuous counterpart (ΔR ~ 0.3 nm) demonstrating a flat uniform surface with the height of surface inhomogeneities of less than 2 nm (Fig. 2c).

The determination of the phase composition of both continuous and porous as-deposited IrMn/[Co/Pd] films was carried out by analyzing their grazing incidence XRD patterns shown in Fig. 2e-f. The main peaks from the phases that compose the MLs are located in the range of diffraction angles 2θ between 38º and 43º represented in the figures. The majority of the peaks can be resolved in the experimental XRD patterns despite their partial overlapping, with a good coincidence of their positions being observed for the two films (dash lines in Fig. 2e-f).

ACCEPTED MANUSCRIPT
Journal of Applied Physics
AIP Publishing
This is the author's peer reviewed, accepted manuscript. However, the online version of record will be different from this version once it has been copyedited and typeset.
PLEASE CITE THIS ARTICLE AS DOI: 10.1063/5.0006194

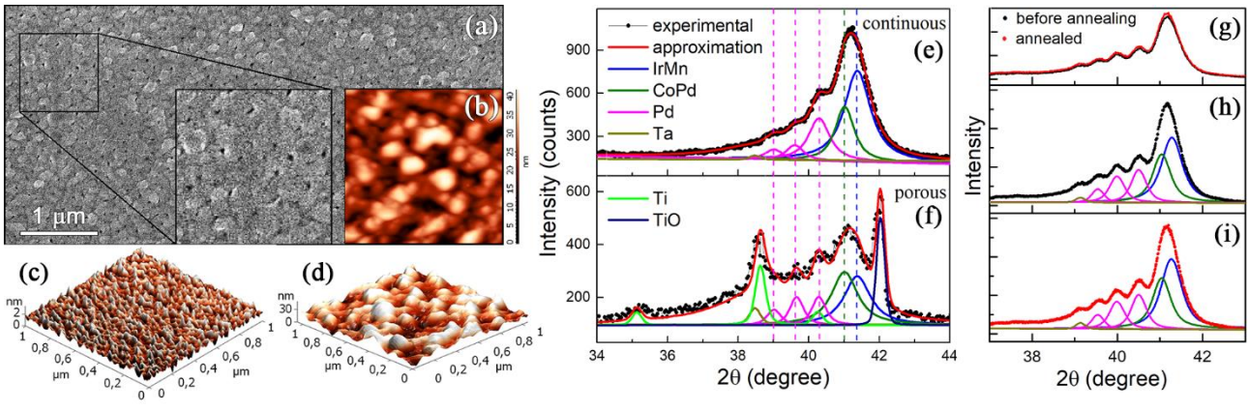

Fig. 2. SEM (a), AFM (b-d) and XRD (e-i) characterization of IrMn/[Co/Pd] films: (a-b) top-view SEM (a) and AFM (b) images of the porous film; (c-d) 3D AFM images of the continuous (c) and porous (d) films; (e-f) parts of grazing incidence XRD patterns of the continuous (e) and porous (f) films; (g-i) parts of theta-theta XRD patterns of the as-deposited (h) and annealed (i) continuous films, and both of these films (g) combined for comparison. Experimental (points) XRD data are accompanied by their approximation (red solid lines) and the corresponding phase decomposition (color lines).

The approximation of the XRD patterns allows identification of the peaks at 2θ = 41.34° and 40.98° corresponding to the (111) plane in face-centered cubic (*fcc*) lattices of $IrMn_3$ phase (a = 3.780 Å)[37] and CoPd alloy (a = 3.811 Å). The latter phase arises as a result of the commonly observed mixing of Co and Pd layers at their interfaces[19,38,39]. The mixing is supposed to be complete, since the obtained lattice constant a of this phase is consistent with that for $CoPd_2$ alloy[41], i.e. the atomic ratio of Co and Pd in the formed alloy is close to the ratio of the thicknesses of the deposited Co and Pd layers. Next, three detected peaks at 2θ = 40.26°, 39.60° and 38.99° relate to the phases with the same *fcc* structure and a slightly different lattice constant (a = 3.877-3.998 Å), with all of them corresponding to Pd modifications[41,42] with somewhat changing cell parameter (PDF#01-087-0638; -0641; -0637). The detected diffraction peaks of Pd are believed to relate mainly to the seed and capping Pd layers. A few revealed Pd modifications can be attributed to tuning the lattice parameter of Pd to be consistent with the lattices of the adjacent layers. Namely, the deposition of the seed Pd layer over the Ta layer with a mismatched lattice leads to a strained Pd lattice with an increased a parameter. Inversely, the deposition of the capping Pd layer over the layer of CoPd alloy with a smaller unit cell provides its reduced a parameter. Besides the above mentioned peaks, the XRD pattern of the porous IrMn/[Co/Pd] film (Fig. 2f) contains the intense diffraction peaks at 2θ = 38.62º and 42.04º, which correspond to Ti and TiO phases, respectively, originating from the template[19,43].

ACCEPTED MANUSCRIPT
Journal of Applied Physics
AIP Publishing
This is the author's peer reviewed, accepted manuscript. However, the online version of record will be different from this version once it has been copyedited and typeset.
PLEASE CITE THIS ARTICLE AS DOI: 10.1063/5.0006194

In order to investigate an effect of annealing on the structure and phase composition of the studied IrMn/[Co/Pd] films, they were analyzed by SEM, AFM and XRD before and after short-term heating (1 min) at T_a = 500 K. No detectable changes in the films morphology are observed by SEM and AFM methods, thus indicating a stability of such films parameters as pore diameter and surface roughness due to a relatively low temperature and short period of thermal treatment. The only noticeable annealing-induced change is observed in the theta-theta XRD patterns of the continuous IrMn/[Co/Pd] film shown in Fig. 2g-i, which relates to a slight increase in the intensity of the peak corresponding to the phase of CoPd alloy possibly occurring due to some thermally-induced ordering of its crystalline structure, with the difference being minimal. Therefore, the described above phase composition and morphology characterizes both as-deposited and annealed films, with no substantial difference being observed. Taking into account thermal stability (T_a = 500 K) of the morphology and phases in the studied films, the described below annealing-induced changes in the magnetic properties of the films are associated only with their magnetic ordering.

B. Magnetic properties: field-cooling effect

For an exhaustive analysis of exchange coupling between FM and AFM layers, the hysteresis loops were measured at different temperatures (T = 10-300K) for both as-deposited and annealed IrMn/[Co/Pd] films. The normalized magnetization curves $M(H)/M_S$ obtained at RT are shown in Fig. 3 for the continuous (a) and porous (b) films. It should be mentioned that the $M(H)/M_S$ dependences for both as-deposited systems were measured at RT two times, i.e. the first curve was obtained just after the films deposition and the second one was measured after some period of time (non-defined exactly, but comparable to a month), i.e. after the films relaxation, and then the set of the curves at different temperatures was measured after ZFC procedure. In doing so, three RT magnetization curves are presented in Fig. 3a,b for each film, namely, for its *as-deposited*, *relaxed* and *annealed* sample.

As can be observed from Fig. 3a, the as-deposited continuous IrMn/[Co/Pd] film demonstrates very close to zero exchange bias that indicates either the absence of the exchange interaction between its AFM and FM layers or such an interaction, which does not shift the corresponding magnetization curve at RT. Additionally, we should take into consideration the fact of a huge increase in H_C parameter equaled now to 970 Oe (RT) with respect to the corresponding films without IrMn layer (655 Oe) or with the inverse layer order, i.e. [Co/Pd]/IrMn film (550 Oe)[19]. In order to understand

ACCEPTED MANUSCRIPT
Journal of Applied Physics
AIP Publishing
This is the author's peer reviewed, accepted manuscript. However, the online version of record will be different from this version once it has been copyedited and typeset.
PLEASE CITE THIS ARTICLE AS DOI: 10.1063/5.0006194

these simultaneously appeared phenomena, namely, an increased H_C parameter and the absence of exchange bias ($H_E \sim 0$), we should consider different possibilities for their combined realization. First of all, a relatively thick IrMn layer (6 nm) can simply play a passive role of a seed layer with the appropriate crystalline structure (*fcc*) and orientation (111). In combination with the Pd seed layer of 3 nm, they can form a common seed layer with a total thickness of 9 nm for the following Co/Pd layer. The corresponding studies shows that an increase in the thickness of the Pd seed layer to 10 nm improves the H_C parameter of the Co/Pd film up to 1025 Oe that is very close to the obtained H_C value of the currently studied IrMn/[Co/Pd] film.

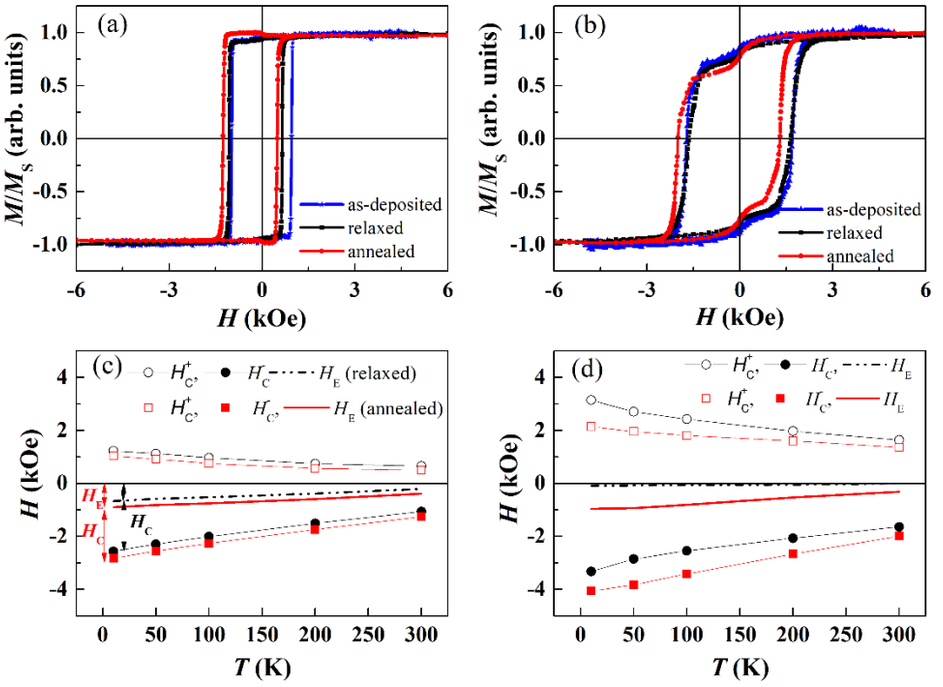

Fig. 3. Parts of the field dependences of the normalized magnetization $M(H)/M_S$ of the continuous (a) and porous (b) IrMn-Co/Pd films measured at $T = 300$ K for as-deposited, relaxed and annealed samples, as well as the temperature dependences of the coercive ($H_C = (H_C^+ - H_C^-)/2$) and exchange bias ($H_E = (H_C^+ + H_C^-)/2$) fields of the continuous (c) and porous (d) IrMn-Co/Pd films obtained for the relaxed (dash-dot black line) and annealed (solid red line) samples.

In doing so, the absence of exchange interaction between Co/Pd and IrMn layers is admissible and can be realized in the case of mismatch in the orientations of magnetic moments in these two layers, e.g. their orthogonal mutual orientation, since IrMn is known to tend to align spins in the film plane[10,25,37,44], or in the case of random domains orientation in IrMn[4]. Indeed, in the case of the previously studied [Co/Pd]/IrMn films[19,45], the IrMn top layer is deposited over the uniformly

ACCEPTED MANUSCRIPT
Journal of Applied Physics
AIP Publishing
This is the author's peer reviewed, accepted manuscript. However, the online version of record will be different from this version once it has been copyedited and typeset.
PLEASE CITE THIS ARTICLE AS DOI: 10.1063/5.0006194

magnetized Co/Pd layer with a huge perpendicular anisotropy (H_a ~ 25 kOe), which aligns spins in AFM material collinearly to FM magnetic moments, at least in the near-interface region. The induced ordering conserves after deposition due to the strong FM-AFM coupling[19]. In the case of the currently studied IrMn/[Co/Pd] films, the Co/Pd layer deposited over the IrMn layer with either randomly or in-plane oriented anisotropy can organize itself as a multi-domain structure either with the equivalent "up" and "down" domains or with the domination of one type of domains due to the presence of a stray field from the magnetron gun (let us conventionally determine the dominant domains as "up" ones for convenience, i.e. as the corresponding to a positive H direction; however, it should be mentioned that in practice the preferred orientation of magnetic moments is stated to be downward[4,23]). The domains imbalance is more expected in our case, because of the evident exchange bias appeared in the as-deposited [Co/Pd]/IrMn films[19], which is believed to be due to such a stray field.

On the other hand, it is known that the AFM spin structure is drastically altered after the deposition of highly anisotropic FM layer on top. Due to an interplay between PMA of Co/Pd domains and in-plane anisotropy of IrMn domains, interfacial spins are partly canted[10,44], but both in "up" and "down" directions in conformity with the domain pattern of the CoPd layer[10,46]. In doing so, two exchange-biased systems can be formed with two opposite orientations of unidirectional anisotropy ("up" and "down")[10,46]. Again, they can be conventionally equivalent[10,46], or one of them is dominating[4,23,47]. The absence of a shift of the corresponding $M/M_S(H)$ curve in this case can be the evidence of (*i*) equivalent shifts of two sub-loops corresponding to "up" and "down" domains in two opposite H directions that is confirmed by an increased H_C value. Alternatively, it can be related to (*ii*) a very thin sub-layer of IrMn which contains tilted magnetic moments coupled with the moments of the FM layer. In the latter case, when the thickness of the coupled IrMn sub-layer is less than 3 nm, the exchange-bias shift is known to be blocked at RT, since T_B determining its occurrence lies bellow than T = 300 K[6]. Being unable to keep the constant orientation, AFM spins can even be rotated together with the FM layer, thus increasing the H_C value but providing zero bias of the corresponding magnetization curve[14].

For choosing the correct explanation of the observed phenomena, low temperature study of the magnetization reversal was carried out, starting with repeating the RT magnetization curve. It unexpectedly shows a significant EB shift equaled to -206 Oe (Fig. 3a) which indicates some relaxation effects occurring with time at the AFM/FM interface[13], since no additional treatment of the sample was applied after its deposition. The observed shift increases significantly with T decrease,

ACCEPTED MANUSCRIPT
Journal of Applied Physics
AIP Publishing
This is the author's peer reviewed, accepted manuscript. However, the online version of record will be different from this version once it has been copyedited and typeset.
PLEASE CITE THIS ARTICLE AS DOI: 10.1063/5.0006194

achieving -668 Oe at T = 10 K. Thus, an evident exchange interaction at the AFM/FM interface, which intensifies at low temperatures, is revealed in the relaxed IrMn/[Co/Pd] film. Domination of one type of FM-domains is now evident in this film due to the observed shift of the hysteresis loop. Since there is no reason for breaking balance between "up" and "down" domains with time without any contributing conditions (heating in an external field, etc.), we can conclude the initial dominance of one type of FM domains (due to a stray field of the magnetron gun), with subsequent reorientation of Mn magnetic moments with time under the influence of the anisotropy field of the Co/Pd layer.

Next, the magnetization curves of the annealed continuous IrMn/[Co/Pd] film were measured at different temperatures. The annealing (T_a = 500 K) has been carried out in a magnetic field of 5 kOe oriented perpendicularly to the film plane. In this case, even RT absolute value of H_E field increases significantly, reaching 384 Oe, which is almost two times higher than the corresponding parameter of the relaxed film. In doing so, the observed increase in H_E value after annealing is associated with more extended or even complete IrMn magnetic ordering in the direction of the film normal[44]. It should be additionally mentioned that the corresponding [Co/Pd]/IrMn film with the same composition but the inverse position of the AFM and FM layers demonstrates, first of all, very close to each other values of H_E before and after annealing, and secondly, this value is two times lower (-179 Oe[19,45]) than the parameter of the currently studied IrMn/[Co/Pd] film. Such a drastic difference conserves at low temperatures, where H_E achieves only -399 Oe for the [Co/Pd]/IrMn film at T = 10 K[19] and reaches -899 Oe for the IrMn/[Co/Pd] counterpart (Fig. 3c). This difference is rather unexpected, especially in the case of low T, because both films contain an identical interface between the IrMn and Co/Pd layers, with the coercive field being close for both systems at T = 10 K (1.7 and 1.9 kOe, respectively).

The RT magnetization curves of the porous IrMn/[Co/Pd] film obtained, similarly to the continuous counterpart, for *as-deposited*, *relaxed* and *annealed* samples are presented in Fig. 3b. As it can be seen from the figure, high coercive field (H_C = 1640 Oe) and zero exchange bias field H_E characterizes the magnetization curves of both as-deposited and relaxed porous films which are similar to each other, in contrast to the corresponding curves of their continuous analogs (Fig. 3a). The obtained H_C value is almost two times higher than that for the continuous film due to a complete or partial transformation of a magnetization reversal mechanism which implies pinning the domain walls (DWs) by pores[31] or occurring the rotational mechanism of magnetization reversal in the porous system instead of DWs motion typical of the continuous films[19,30,48]. The exchange bias field of the

ACCEPTED MANUSCRIPT
Journal of Applied Physics
AIP Publishing
This is the author's peer reviewed, accepted manuscript. However, the online version of record will be different from this version once it has been copyedited and typeset.
PLEASE CITE THIS ARTICLE AS DOI: 10.1063/5.0006194

as-deposited porous film, which is nearly zero at RT, remains low at T = 10 K (-92 Oe), that is supposed to be the result of the complex morphology of the film (Fig. 2a-d). Indeed, structural damages and defects of the film near the pores and the corresponding disordering of magnetic moments lead to a weakened magnetic anisotropy of the Co/Pd layer. Thus, a reduced anisotropy field cannot influence so intensively the magnetic moments of the IrMn layer to provide their tilting sufficient for exchange coupling establishing.

The annealing of the porous IrMn/[Co/Pd] film results however in the expected exchange bias shift of the RT magnetization curve (H_E = -315 Oe, Fig. 3b) increasing monotonically up to -960 Oe with decreasing temperature (T = 10 K, Fig. 3d). An increase in H_E at low temperature correlates with H_C increase, which, in turn, is a consequence of PMA enhancement. In doing so, strictly parallel alignment of magnetic moments in the FM layer provides strengthening the interlayer exchange coupling. The maximal H_C value achieves 3.2 kOe for the porous IrMn/[Co/Pd] film at T = 10 K, regardless of the preliminary annealing and the regime of cooling. Inversely, the maximal H_E value equaled to -900-960 Oe is achieved at T = 10 K only for the annealed IrMn/[Co/Pd] films, which were cooled in a magnetic field, independently of their porosity.

One more important peculiarity of the magnetization curves of the porous IrMn/[Co/Pd] film is their step-like shape with the inflection in the vicinity of zero field. Such steps are commonly associated with the complex morphology of the films induced by their porosity or surface irregularities[19,45]. Indeed, the soft-magnetic phase (or soft-magnetic component of the FM layer) which is proved to appear near the pore edges due to the local magnetic disordering[19] demonstrates distinct magnetic parameters including low coercive field and magnetic susceptibility that implies its isotropic magnetic properties. Being similar at room temperature, the shape of the $M(H)/M_S$ curves of the as-deposited and annealed porous IrMn/[Co/Pd] films differs significantly at low temperature. The corresponding low-temperature $M(H)/M_S$ dependences are shown in Fig. 4. As it can be seen from the figure, the steps in the hysteresis loops of the annealed film become more pronounced at $T \leq 200$ K, in contrast to the curves of the as-deposited sample, which demonstrate high similarity at different temperatures. In order to explain such a discrepancy, a model decomposition of the $M(H)/M_S$ curves measured at different temperatures for both porous films studied was carried out in accordance with the procedure described in detail previously[19]. The results of approximation are presented in Fig. 5. Briefly, we have analyzed the positions of maxima of the first derivative of the magnetization curves ($dM(H)/dH$) which correspond to the magnetization reversal of each magnetic phase in the film[49]. The

ACCEPTED MANUSCRIPT
Journal of Applied Physics
AIP Publishing
This is the author's peer reviewed, accepted manuscript. However, the online version of record will be different from this version once it has been copyedited and typeset.
PLEASE CITE THIS ARTICLE AS DOI: 10.1063/5.0006194

global maximum of the d$M(H)$/dH curve (blue line under the d$M(H)$/dH curves in Fig. 5) corresponds to a hard-magnetic component of the FM layer, whereas an additional less-intensive maximum in the vicinity of zero field (green line under the d$M(H)$/dH curves in Fig. 5) relates to a soft-magnetic component of the FM layer.

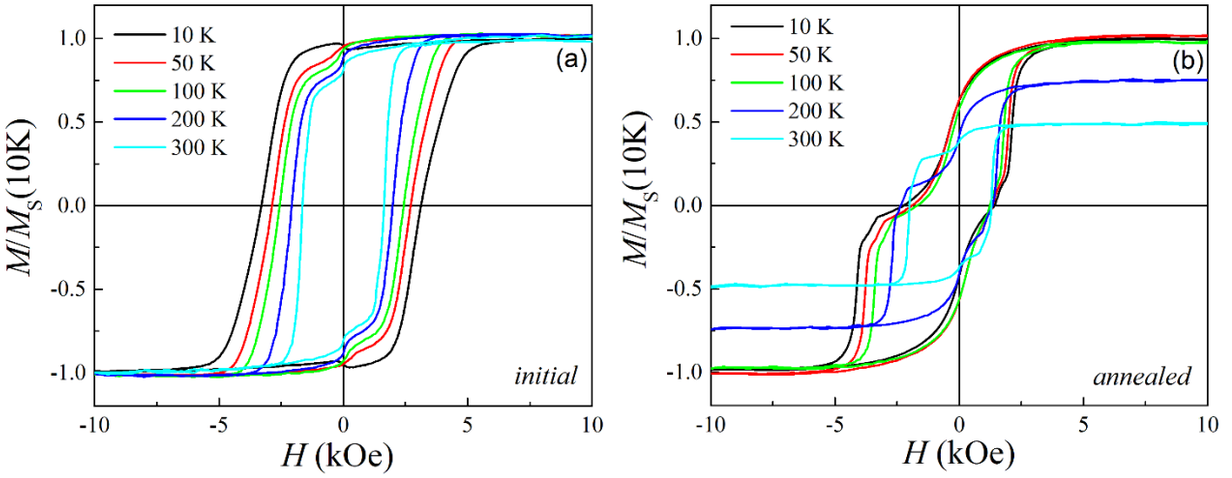

Fig. 4. Parts of the field dependences of normalized magnetization $M(H)/M_S^{10K}$ of the porous IrMn/[Co/Pd] films measured at T = 10-300 K for the as-deposited (a) and annealed (b) samples.

In doing so, the magnetization curves of the porous IrMn/[Co/Pd] films were fitted using the following formula:

$$M(H)/M_S^{10K} = \sum_{i=1}^{2}\left(\frac{M_S^i/M_S^{10K}}{\tanh(k^i\times(H\pm H_C^i))} - \frac{M_S^i/M_S^{10K}}{k^i\times(H\pm H_C^i)}\right), \quad (1)$$

where M_S^{10K} is the saturation magnetization of the whole film at low temperature (10 K), M^i_S is the saturation magnetization at any given temperature, H^i_C is the corresponding coercive field, and k^i is a slope of a magnetization curve related to i = 1, 2 phase. Here, i = 1 is used to represent the hard-magnetic phase, and i = 2 characterizes the soft-magnetic phase. The extracted magnetization curves of each magnetic phase at different T are collected in Fig.5c-f.

First, a significantly different shape of the magnetization curves characterizing hard and soft magnetic components of the porous films is obviously obtained. The former is similar to the $M(H)/M_S$ dependences of the continuous film and the latter is characteristic of an isotropic magnetic system. However, there are some important discrepancies in the corresponding components of the two films, namely, as-deposited and annealed. The main one is the relative contribution of the components. In

ACCEPTED MANUSCRIPT
Journal of Applied Physics
AIP Publishing
This is the author's peer reviewed, accepted manuscript. However, the online version of record will be different from this version once it has been copyedited and typeset.
PLEASE CITE THIS ARTICLE AS DOI: 10.1063/5.0006194

the as-deposited film, the hard-magnetic phase is dominant in the whole temperature range analyzed, while the ratio of these two components changes with temperature in the annealed film. Namely, the almost equal contribution of the soft and hard magnetic components in the total magnetization curves of the annealed film is detected at $T \leq 100$ K (Fig. 5 e,f), whereas a strong dominance of the hard one is characteristic of this film at RT. Additionally, a somewhat different shape of the magnetization curves describing the hard-magnetic phase is revealed for the as-deposited and annealed IrMn/[Co/Pd] films (Figs. 5c and e). While the hard-magnetic component of the annealed film demonstrates the rectangular shape of its $M(H)/M_S$ loops (Fig. 5e), the as-deposited sample shows more tilted curves with respect to $H = 0$ axis (Fig. 5c). The two above-described peculiarities indicate a completely different magnetic moments ordering in the as-deposited and annealed films and consequently, different processes of their magnetization reversal.

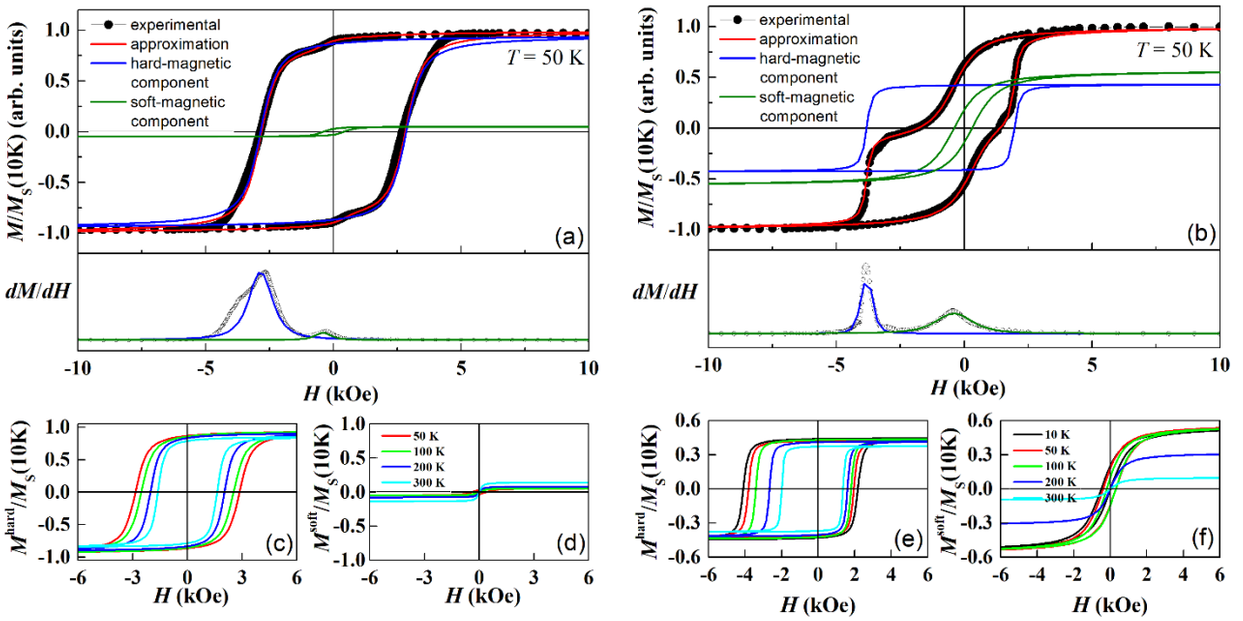

Fig. 5. Hysteresis loops $M(H)/M_S$ of the porous IrMn/[Co/Pd] films, (a) as-deposited and (b) annealed, which are measured at $T = 50$ K, accompanied by their model decomposition into the components corresponding to the hard-magnetic (c, e) and soft-magnetic (d, f) phases at different temperatures ($T = 10$-300 K). The panel below each loop shows the first derivatives of the upper branches of the magnetization curves. Black points in (a, b) represent the experimental data, red solid lines correspond to the fit of the overall loops, whereas blue and green solid lines in (a, b) show sub-loops related to the hard-magnetic and soft-magnetic regions of the films.

ACCEPTED MANUSCRIPT
Journal of Applied Physics
AIP Publishing
This is the author's peer reviewed, accepted manuscript. However, the online version of record will be different from this version once it has been copyedited and typeset.
PLEASE CITE THIS ARTICLE AS DOI: 10.1063/5.0006194

C. Magnetic properties: interfacial ordering

Let us describe consistently the observed phenomena in terms of magnetic ordering at the AFM/FM interface for two different "magnetic phases". The hard-magnetic phase demonstrating a high PMA is formed on flat areas of the template surface which are far from pore edges and free from sharp inhomogeneities. The shape of its $M(H)/M_S$ curves is consistent with the shape of the corresponding curves of the continuous film (compare Figs. 3a and 5e), including the temperature dependences of its H_C and H_E parameters (Fig. 3c). The soft-magnetic phase with predominantly isotropic magnetic properties is formed mainly near the pores. Indeed, since the film covers pore edges and surface inhomogeneities of template with high surface curvature, it contains misaligned magnetic moments with their almost equiprobable orientation. Its magnetization curves thus demonstrate "S-type" shape with, however, significant coercive and exchange bias fields at $T \leq 100$ K, with the latter being characteristic only of the annealed sample (Fig. 5f). High values of low-temperature H_C and H_E parameters (H_E achieves -244 Oe at $T = 10$ K) of the soft-magnetic phase arise obviously from its close contact and coupling with the hard-magnetic phase due to the film continuity, since the film splitting into magnetic phases is conventional. An unexpected fact is a separate magnetization reversal of the connected parts (*hard* and *soft*) within one system, i.e. a continual film. Similar step-like magnetization reversal was previously observed for the porous [Co/Pd]/IrMn films[19] and was discussed in the context of different orientation of FM/AFM exchange interaction in different parts of the film, namely perpendicular exchange bias involving the hard-magnetic phase of the Co/Pd layer and in-plane pinning of magnetic moments of the soft-magnetic phase by IrMn.

Taking into account the peculiarities of the layers position in the currently studied IrMn/[Co/Pd] porous film, the above model should be extended to describe its magnetization reversal. Indeed, the as-deposited porous film does not show any exchange bias either just after deposition or after relaxation. The dominant hard-magnetic phase in this film describes almost the whole FM layer including flat interpore areas and curved near-pore regions, i.e. the FM layer of the film can reverse its magnetic moments as a single unit, ignoring the presence of IrMn. The "tilted" shape of its hysteresis loops (Fig. 5c) and the corresponding "doubled" peak of the $dM(H)/dH$ dependence (Fig. 5a) evidences that the FM material, which is located near the pores, is also included into this "hard-magnetic phase" during the magnetization reversal process.

Next, annealing the porous film in a perpendicular magnetic field is able to induce perpendicular ordering of the interfacial magnetic moments in the regions of IrMn adjacent to the hard-magnetic

ACCEPTED MANUSCRIPT
Journal of Applied Physics
AIP Publishing
This is the author's peer reviewed, accepted manuscript. However, the online version of record will be different from this version once it has been copyedited and typeset.
PLEASE CITE THIS ARTICLE AS DOI: 10.1063/5.0006194

phase of the FM layer, thus initiating their exchange coupling, but it is insufficient to induce similar spins arrangement in the parts of IrMn contacting with the soft-magnetic phase of the FM layer. Inversely, an in-plane exchange coupling is expected between the FM and AFM layers in the latter regions. This assumption is confirmed by the separate magnetization reversal of the part of FM layer, namely the soft-magnetic phase. This phase can be revealed after annealing as a separate component of the $M(H)/M_S$ curve (Fig. 5f). The supposed in-plane ordering can be caused by thermal effect during annealing. Indeed, the applied cooling field H_{FC} = 5 kOe seems to be insufficient for magnetic moments ordering in the initially disordered (or ordered in other direction) AFM layer. The anisotropy field of the Co/Pd layer equaled to ~25 kOe is much higher and can help in such an ordering, but it covers just the regions close to the hard-magnetic phase, which is the source of this field. The areas of IrMn adjacent to the soft-magnetic regions of the FM layer do not undergo such an extra-field influence, but their moments can arrange themselves at the increased temperature ($T > T_N$) in accordance with the intrinsic properties of the AFM layer related to its crystalline structure. As it is shown by the XRD measurements (Fig. 2), the (111) plane of *fcc* $IrMn_3$ phase corresponds to the film plane, thus implying that the majority of Mn magnetic moments are oriented in directions close to this plane[25,37,44,47]. Even being initially disordered or possessing a random domains orientation, the IrMn layer can improve its spins arrangement during the film heating.

In doing so, we can explain the double-step low-temperature magnetization reversal of the annealed porous IrMn/[Co/Pd] film (Fig. 4b) by the competition between two exchange anisotropies, namely a PMA of the FM layer and an in-plane anisotropy of the AFM layer (parts of the layer) determining an in-plane coupling between FM and AFM spins at the interface. The dominance of the latter at RT induces strong pinning of the magnetic moments of the FM soft-magnetic phase by IrMn, even preventing its participation in the magnetization reversal in an external field perpendicular to the film plane (at least, within H less than 10 kOe verified in Fig. 4b). At low T, an increase in PMA of the Co/Pd layer (up to ~35 kOe at 50 K compared to 25 kOe at RT) allows to involve the soft-magnetic phase into magnetization reversal process in a perpendicular external field. However, a separate magnetization reversal of the hard- and soft-magnetic components of the film occurs due to an in-plane coupling of IrMn with the soft-magnetic phase impeding its reversal. Decreasing temperature thus leads to a rapid increase in M_S of the annealed IrMn/[Co/Pd] porous film. The extracted $M_S(T)/M_S^{max}$ dependences of this film and separately of its hard-magnetic component are shown in Fig. 6 accompanied by their approximation using the Bloch's $T^{3/2}$ law[50]. Since the saturation

ACCEPTED MANUSCRIPT
Journal of Applied Physics
AIP Publishing
This is the author's peer reviewed, accepted manuscript. However, the online version of record will be different from this version once it has been copyedited and typeset.
PLEASE CITE THIS ARTICLE AS DOI: 10.1063/5.0006194

magnetization of the whole porous film is the sum of the magnetizations of the two components, the common hysteresis loop was fitted using the two-component formula[50]:

$$M_S(T)/M_S(0) = n \times \left(1 - \left(\frac{T}{T_C}\right)^{\frac{3}{2}}\right) + (1-n) \times \left(1 - \left(\frac{T}{T_b}\right)^{3/2}\right), \quad (2)$$

where $M_S(0)$ is the saturation magnetization of the whole film at T = 0 K, n and (1-n) are the contributions of the hard- and soft-magnetic phases, respectively, T_C is the Curie temperature of the hard magnetic phase, and T_b determines the blocking temperature of the soft magnetic phase. First, T_C was determined from the approximation of $M_S(T)$ dependence of the hard-magnetic component, which was found to be 980 K. The obtained T_C value corresponds well to the similarly estimated parameter of the continuous film (1160 K) and is rather close to that for other Co-Pd systems, i.e. it is somewhat decreased with respect to T_C value of bulk *fcc* Co (1388 K[51]) due to the alloying with Pd[52] and low layer thickness, but it even exceeds the T_C values obtained for close Co/Pd MLs (750 K[53]).

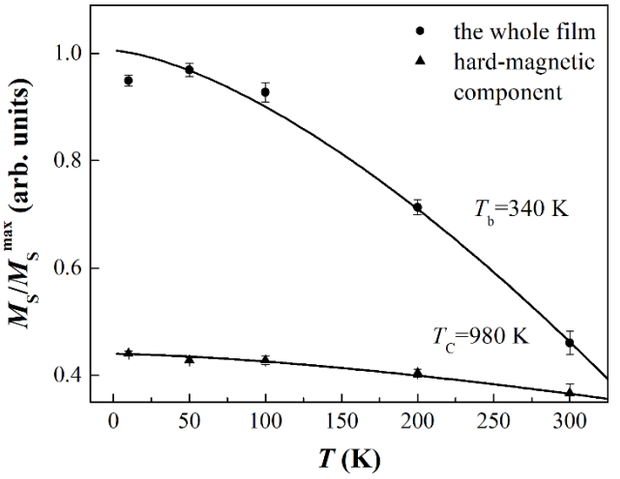

Fig. 6. Temperature dependences of normalized saturation magnetization $M_S(T)/M_S^{max}$ of the annealed porous IrMn/[Co/Pd] film obtained from the experimental magnetization curves $M(H)$ (circles) and from the extracted hard-magnetic component $M^{hard}(H)$ (triangles), accompanied by their approximation (solid lines) using the Bloch's $T^{3/2}$ law.

However, T_b parameter characterizing the soft-magnetic phase, which is extracted from the fit of the total magnetization curve (Fig. 6), is found to be 340 K only, thus indicating that the rapid decrease in M_S of the porous film with increasing T is caused by the difference in the transition temperatures of the two magnetic components. The magnetization of the soft one thus becomes zero at T = 340 K, i.e. its magnetic moments are supposed to be blocked along the in-plane direction at

ACCEPTED MANUSCRIPT
Journal of Applied Physics
AIP Publishing
This is the author's peer reviewed, accepted manuscript. However, the online version of record will be different from this version once it has been copyedited and typeset.
PLEASE CITE THIS ARTICLE AS DOI: 10.1063/5.0006194

$T > T_b$. Another possible reason of M nulling lies in increased temperature fluctuations reducing rapidly the magnetization of small (superparamagnetic) nanostructures, which can contribute to the soft-magnetic component of the film[49].

To choose between the above alternatives, the magnetization curves of the porous IrMn/[Co/Pd] film were obtained in (*i*) a high perpendicular external field (up to 9 T) intended for breaking strong in-plane pinning effect (Fig. 7a) and (*ii*) an in-plane magnetic field (Fig. 7b). It should be mentioned that both presented series of the curves were measured for the annealed sample after some period of relaxation after annealing, i.e. somewhat later than the previous, *as-annealed*, $M(H)$ curves (Fig. 4b).

First of all, the absence of the exchange bias is detected in the direction normal to the film plane (Fig. 7a), despite the FC procedure applied. This indicates the reduction of the PEB coupling between FM and AFM layers possibly arising from the reorientation of IrMn magnetic moments back, towards the in-plane direction. Thus, the shape of RT magnetization curve of the annealed film in the direction normal to the film plane (inset in Fig. 7a) is now similar to that obtained before annealing (Fig. 4a).

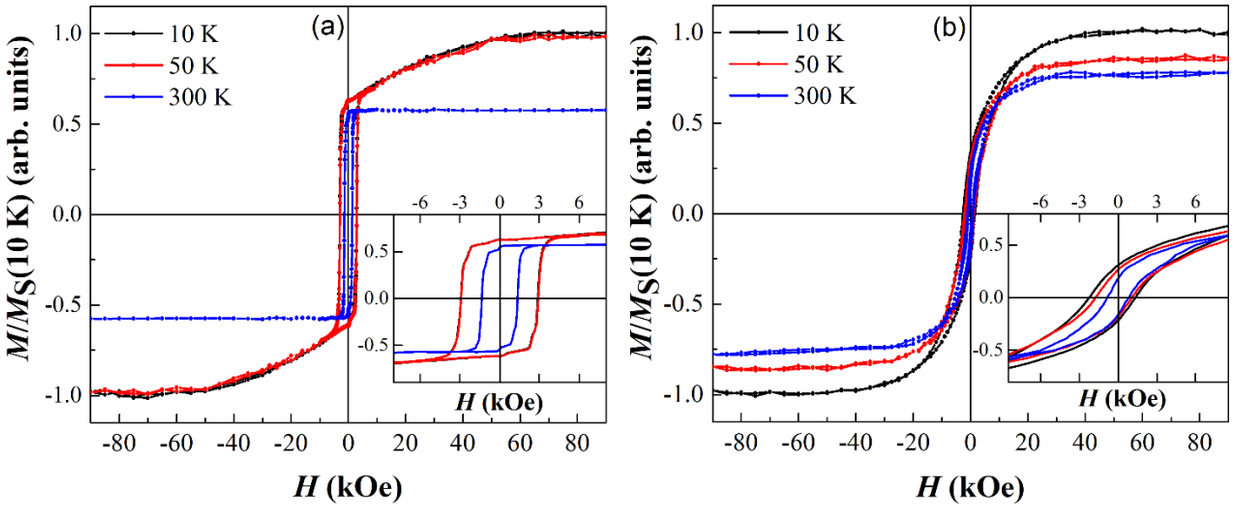

Fig. 7. Field dependences of normalized magnetization $M(H)/M_S^{10K}$ of the annealed porous IrMn/[Co/Pd] film measured at T = 10-300 K in the directions normal to the film plane (a) and along the film plane (b). The insets represent the enlarged central parts of the curves.

The most important peculiarities are characteristic of the low-temperature magnetization curves of the annealed porous IrMn/[Co/Pd] film in H > 10 kOe (Fig. 7a). On the one hand, there are no steps which were observed for the low-temperature $M(H)/M_S$ dependences of the as-annealed film (Fig. 4b). However, a gradual increase in the magnetization is detected up to saturation, which is significantly

ACCEPTED MANUSCRIPT
Journal of Applied Physics
AIP Publishing
This is the author's peer reviewed, accepted manuscript. However, the online version of record will be different from this version once it has been copyedited and typeset.
PLEASE CITE THIS ARTICLE AS DOI: 10.1063/5.0006194

higher than the corresponding RT parameter (Fig. 7a). It should be mentioned, that the relative increase in M_S parameter with reducing T is comparable to that for the as-annealed film (Fig. 6). At the same time, the in-plane magnetization curves of the porous film relaxed after annealing (Fig. 7b) demonstrate the EB shift at $T < 300$ K reaching -448 Oe at 10 K. The shape of the central part of the in-plane curves showing high H_C parameter (up to 1.8 kOe) and high magnetic susceptibility (inset in Fig. 7b) clearly indicates that a significant part of the FM layer obeys the in-plane anisotropy. Importantly, an increase in M_S with decreasing temperature is not so high in H applied along the film plane (Fig. 7a), as along its normal (Fig. 7b), with the rapid increase being at $T < 50$ K. The observed phenomena integrally reveal that a large part of magnetic moments of the FM layer is pinned along the in-plane direction, with the coupling being strong enough to overcome the influence of perpendicular external field at RT. Being an isotropic phenomenon, superparamagnetism can be excluded from the discussion, since the observed increase in M_S with decreasing T is different by value for different field orientations.

Based on the whole array of the obtained data on the magnetization reversal of the IrMn/[Co/Pd] films, we can propose a schematic representation of the spins ordering at the AFM/FM interface under different external conditions for both continuous and porous films. The corresponding scheme is shown in Fig. 8.

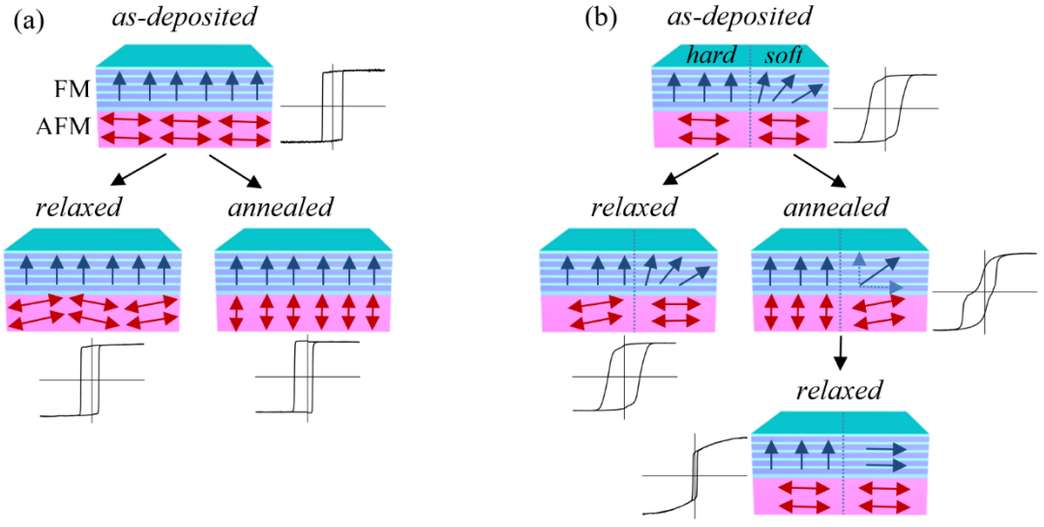

Fig. 8. Schematic representation of the magnetic ordering at the AFM/FM interface in the continuous (a) and porous (b) IrMn/[Co/Pd] films under different external conditions (after deposition, relaxation and annealing), accompanied by the parts of the corresponding $M(H)/M_S$ dependences (see text).

ACCEPTED MANUSCRIPT
Journal of Applied Physics
AIP Publishing
This is the author's peer reviewed, accepted manuscript. However, the online version of record will be different from this version once it has been copyedited and typeset.
PLEASE CITE THIS ARTICLE AS DOI: 10.1063/5.0006194

It should be mentioned that the sketches illustrate the magnetic ordering within only one domain in the FM layer ("up" domain) for simplicity. However, it is understood that two types of domains with the opposite orientation of magnetic moments can be formed. All the described states of the films represented in Fig. 8 are accompanied by typical magnetization curves. For the continuous films in Fig. 8a, the $M(H)$ dependences are presented in the H range of 5 kOe at RT. For the porous films in Fig. 8b, the magnetization curves are shown in the H range of 9 kOe (only the last one within H = 70 kOe) at T = 50 K for better visualization of the observed peculiarities.

Summarizing the proposed sequences, which demonstrate the changes in magnetic moments arrangement at the AFM/FM interface, the influence of the field cooling and the films' porosity can be easily revealed. In doing so, the perpendicular exchange coupling is preferable for the continuous IrMn/[Co/Pd] films with strong PMA. The coupling is enhanced after annealing in a perpendicular external field and is stable with time. Inversely, the porous films demonstrate the tendency to form the exchange coupling oriented along the film plane, with the effect of annealing in perpendicular field being unstable.

D. Magnetoresistance

Magnetoresistive properties of both continuous and porous IrMn/[Co/Pd] films were studied in comparison with the corresponding magnetization curves, i.e. taking into account magnetic moments ordering in the FM layer. The field dependences of magnetoresistance $\Delta R(H)/R_0$ and magnetization $M(H)/M_S$ of the continuous and porous IrMn/[Co/Pd] films measured at different temperatures in a magnetic field perpendicular to their surface are presented in Figs. 9 and 10. Both sets of the curves are obtained for the relaxed samples, i.e. for the as-deposited films after some period of relaxation.

As it is clear seen from Fig. 9, a negative magnetoresistance is characteristic of the continuous film with an almost linear non-saturated field dependence at different temperatures, thus implying that magnon magnetoresistance (MMR) is the dominant mechanism of field-dependent electrons scattering in the film[19,54,55]. In doing so, a field-induced damping of spin-waves determines the shape of the $\Delta R(H)/R_0$ curves. Next, an evident correlation of $\Delta R(H)/R_0$ and $M(H)/M_S$ curves is detected for the continuous IrMn/[Co/Pd] film in low fields close to the H_C value at different temperatures (Fig. 9), thus demonstrating a high sensitivity of electrons scattering to the domain walls formed during the magnetization reversal process[19,56].

ACCEPTED MANUSCRIPT
Journal of Applied Physics
This is the author's peer reviewed, accepted manuscript. However, the online version of record will be different from this version once it has been copyedited and typeset.
PLEASE CITE THIS ARTICLE AS DOI: 10.1063/5.0006194
AIP Publishing

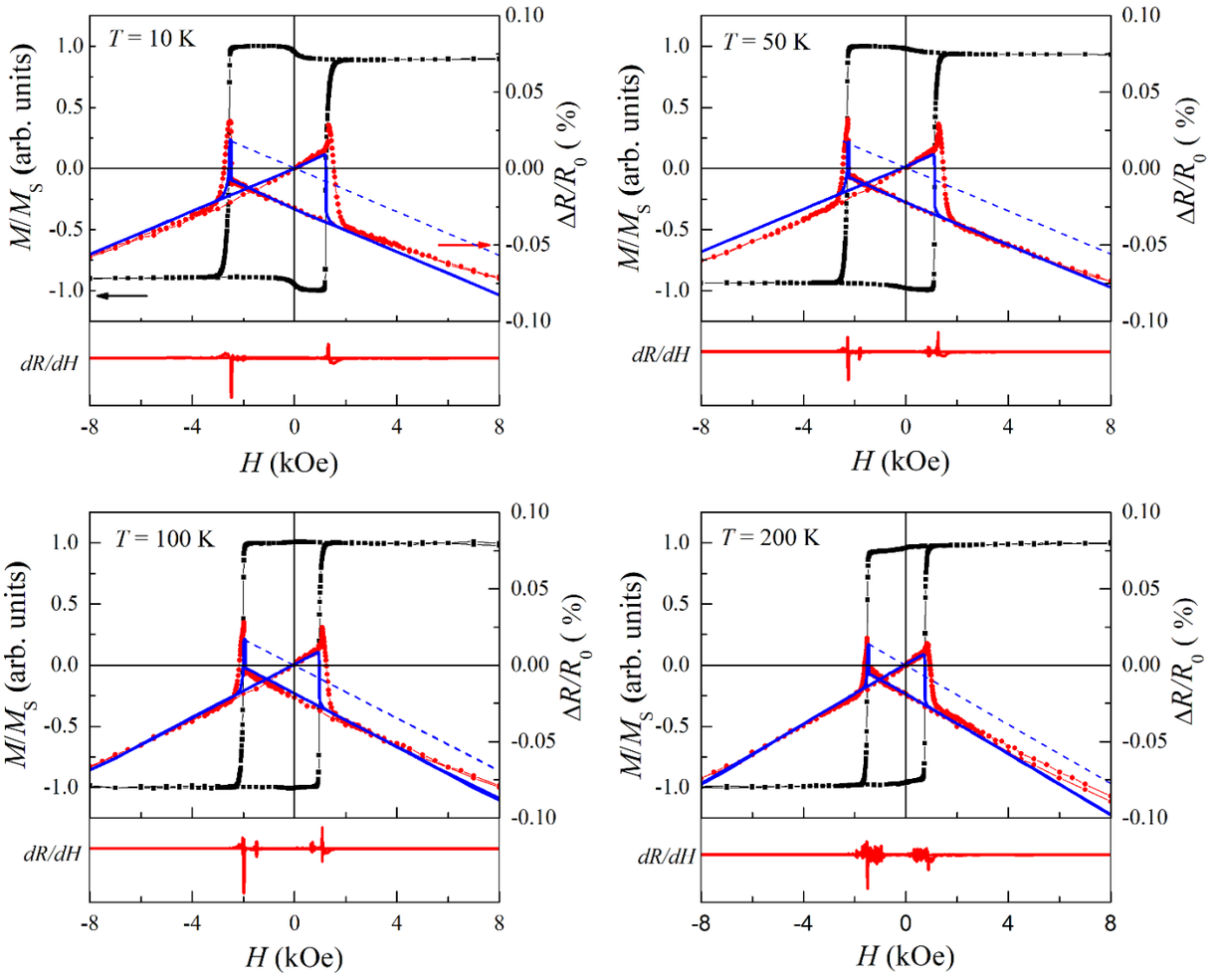

Fig. 9. Field dependences of magnetization $M(H)/M_S$ (black squares) and magnetoresistance $\Delta R(H)/R_0$ (red circles) of the continuous IrMn/[Co/Pd] films measured at different temperatures T = 10-200 K. Blue solid lines represent the approximation of the experimental $\Delta R(H)/R_0$ dependences, blue dash lines correspond to the symmetric position of the left and right branches of the $\Delta R(H)/R_0$ dependences in the opposite external fields. The panel below each curve shows the first derivative $dR(H)/dH$ (red solid line) of the experimental $R(H)$ dependences.

According to the model describing the MMR mechanism[55], the approximation of $\Delta R(H)/R_0$ dependences can be carried out in the low-field range using the corresponding magnetization curves $M(H)/M_S$ with the next formula:

$$R(H) = -\frac{M(H)}{M_S}\alpha(T)H, \quad (3)$$

ACCEPTED MANUSCRIPT
Journal of Applied Physics
AIP Publishing
This is the author's peer reviewed, accepted manuscript. However, the online version of record will be different from this version once it has been copyedited and typeset.
PLEASE CITE THIS ARTICLE AS DOI: 10.1063/5.0006194

where $M(H)/M_S$ corresponds to the magnetization curve of the film measured at the same temperature as $R(H)$ dependence, and $\alpha(T) = (\delta\Delta R(T)/\delta H)_{H\to 0}$ is the absolute value of a slope of $\Delta R(H)$ dependence in the vicinity of zero field. The results of fitting accompany the experimental $\Delta R(H)/R_0$ dependences in Fig. 9.

A good coincidence of the approximating curves with the experimental results confirms a strong correlation between the magnetoresistance of the studied film and the ordering of magnetic moments in the FM layer. Since the AFM layer influences the moments in the FM layer during the magnetization reversal process, pinning them along a certain direction, a related horizontal shift of the $\Delta R(H)/R_0$ dependences arises, reproducing a bias shift of the corresponding $M(H)/M_S$ curves. The main discrepancy between the experimental and approximating curves is a slight vertical shift of the left and right branches of the experimental $\Delta R(H)/R_0$ dependences with respect to each other, which is not predicted by eq. (3) (dash lines in Fig. 9). According to our previous observation for the [Co/Pd]/IrMn film[19], such a shift is associated with its unidirectional magnetic anisotropy. Indeed, a slightly decreased resistance in a positive external field (corresponds to the orientation of unidirectional anisotropy) relates to a reduced angle of precession of spins in the FM layer pinned by AFM spins in this direction. Inversely, an increased resistance in a negative external field is due to an increased angle of spins precession in the FM layer stimulated by their coupling with AFM spins forcing their reversal.

Figure 10 shows the $M(H)/M_S$ and $\Delta R(H)/R_0$ dependences of the porous IrMn/[Co/Pd] film. As can be seen from the figure, the peaks of $\Delta R(H)/R_0$ dependences are broadened significantly, as compared to those of the continuous counterpart, since the magnetization reversal process is less sharp in the porous film containing soft-magnetic regions and thus demonstrating a reduced PMA. The field dependences of the first derivative of the $R(H)$ curves additionally shown in Fig. 10 clearly illustrate the delayed process of magnetization reversal in the porous system, with a good correspondence of the ranges with non-constant dR/dH values to the "tilted" parts of the $M(H)$ curves in the vicinity of H_C. The porous morphology of the film and the corresponding pinning effects implies a higher density of DWs during magnetization reversal[57] and canting the magnetic moments near the pores. As a result, the magnetoresistance in a low field is mainly determined by the electrons scattering on DWs or on the canted magnetic moments of the near-pore regions of the film.

ACCEPTED MANUSCRIPT
Journal of Applied Physics
AIP Publishing
This is the author's peer reviewed, accepted manuscript. However, the online version of record will be different from this version once it has been copyedited and typeset.
PLEASE CITE THIS ARTICLE AS DOI: 10.1063/5.0006194

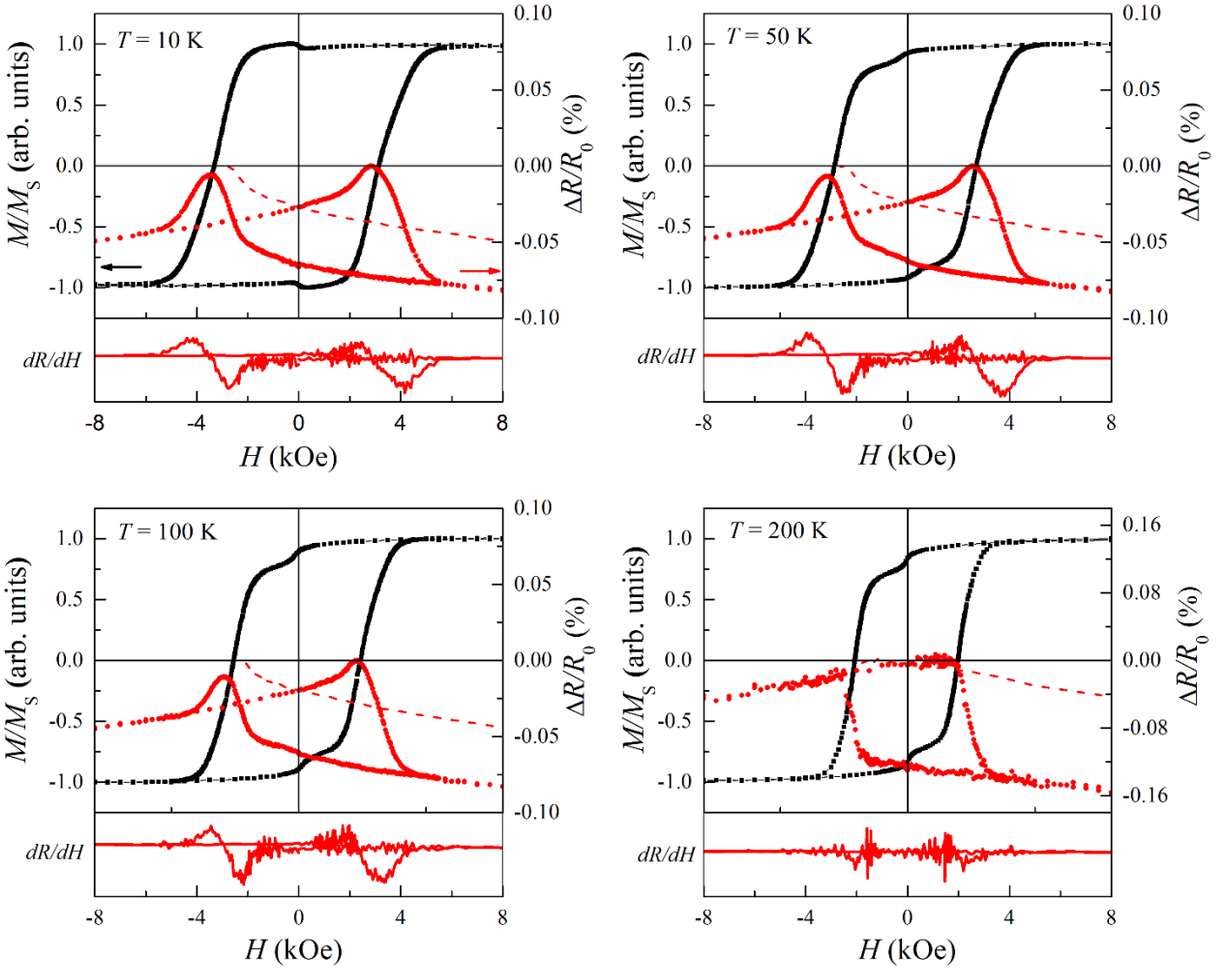

Fig. 10. Field dependences of magnetization $M(H)/M_S$ (black squares) and magnetoresistance $\Delta R(H)/R_0$ (red circles) of the porous IrMn/[Co/Pd] films measured at different temperatures T = 10-200 K. Red dash lines correspond to the symmetric position of the left and right branches of the $\Delta R(H)/R_0$ dependences in the opposite external fields. The panel below each curve shows the first derivative $dR(H)/dH$ (red solid line) of the experimental $R(H)$ dependences.

Besides the broad maxima, an increased asymmetry of the left and right branches of the $\Delta R(H)/R_0$ dependences reaching 0.12% is characteristic of the porous IrMn/[Co/Pd] film, as compared to its continuous counterpart (0.02%), with the asymmetry being increased with temperature (Fig. 10). Being an origin of such an asymmetry in the continuous film, the unidirectional magnetic anisotropy cannot explain a similar phenomenon in the porous system completely, since its unidirectional anisotropy is much weaker than that of the continuous counterpart. The exchange bias shift, as a measure of the unidirectional anisotropy, is significantly lower for both $M(H)/M_S$ (Fig. 3b) and $\Delta R(H)/R_0$ (Fig. 10) curves of the porous film than that of the continuous one. The explanation is

ACCEPTED MANUSCRIPT
Journal of Applied Physics
AIP Publishing
This is the author's peer reviewed, accepted manuscript. However, the online version of record will be different from this version once it has been copyedited and typeset.
PLEASE CITE THIS ARTICLE AS DOI: 10.1063/5.0006194

believed to be connected with the soft-magnetic areas in the FM layer of the porous film. Previously, similar increased asymmetry was detected in the porous [Co/Pd]/IrMn films with the inverse position of the FM and AFM layers[19], which was explained by the combined effect of the reduced PMA of the FM layer in the porous system and the in-plane anisotropy of the IrMn layer[25,37,44,47]. As a result, a partial rotation of the magnetic moments of the AFM layer which follow the FM spins was assumed in the magnetization reversal process[19,47]. Their rotation is limited by the positions normal and parallel to the film plane. The former, being collinear to FM spins, leads to a decrease in the film's resistance, while the latter induces high-resistive state of the film due to the perpendicular mutual orientation of FM and AFM spins, thus impeding the current propagation through the top AFM layer.

A bottom position of the IrMn layer in the present study does not allow a complete application of this explanation, since the electric current can ignore the bottom IrMn layer without penetrating inside it. However, flowing just in the FM layer, it scatters from the AFM/FM interface, with at least its partial penetration into the metallic AFM layer being not excluded. In doing so, the interfacial ordering of magnetic moments of both layers is particularly important in the formed MR signal of the IrMn/[Co/Pd] films. Thus, splitting the FM layer of the porous film into the hard- and soft-magnetic regions appears in different properties of the adjacent areas of the underlying AFM layer. Part of the layer undergoes strong influence of the anisotropy field of the hard-magnetic phase of the FM layer, which induces tilting these AFM magnetic moments towards perpendicular to the film plane direction, whereas the rest of the AFM layer is free from such an influence (Fig. 8b). Such a splitting with the alternation of these regions with a nanoscale period (~50 nm) makes it easier to rotate the interfacial spins of part of the AFM layer coupled with the hard-magnetic phase during magnetization reversal of the FM layer. Thus, the difference between the values of the resistance in similar, but opposite external fields can be attributed to the difference in the angle between the FM and AFM magnetic moments. The latter are supposed to be tilted upward when the external field is oriented along the unidirectional perpendicular anisotropy of the FM layer and are aligned in the film plane in the opposite field. The reduced asymmetry of the $\Delta R(H)/R_0$ dependences with decreasing T (Fig. 10) is thus related to a decrease in temperature fluctuations of magnetic moments, which facilitate the rotation of the AFM spins, as well as to an increase in the in-plane anisotropy of the AFM layer, which complicates such a rotation.

ACCEPTED MANUSCRIPT
Journal of Applied Physics
AIP Publishing
This is the author's peer reviewed, accepted manuscript. However, the online version of record will be different from this version once it has been copyedited and typeset.
PLEASE CITE THIS ARTICLE AS DOI: 10.1063/5.0006194

IV. CONCLUSION

We have carried out a detailed analysis of the magnetization reversal process in the IrMn/[Co/Pd] films with high PMA in dynamics, starting with their deposition, after a period of relaxation, and including subsequent annealing in a magnetic field. A significant difference is detected for the formed exchange bias in the continuous and nanoporous films related to a difference in their morphology. An exceedingly high coercive field reaching 0.9 kOe and 1.7 kOe for the continuous and porous as-deposited films at RT, as well as their nearly zero EB shift are found to be the peculiarities of the bottom position of the IrMn layer, which initially possesses an in-plane anisotropy. An extremely strong perpendicular anisotropy of the Co/Pd layer ($H_a \sim 2.5$ kOe) is able, however, to change progressively the orientation of magnetic anisotropy in the adjacent region of the AFM layer, thus inducing a significant PEB (-200 Oe at RT) in the continuous film, but is insufficient to cause PEB in the porous film without an additional in-field annealing. Application of such annealing intensifies considerably the exchange coupling in the continuous film, increasing its PEB (up to -384 Oe at RT), and promotes PEB in the porous film (-315 Oe at RT). Due to the presence of the soft-magnetic component in the FM layer of the porous film with the dominating highly-anisotropic hard-magnetic phase, a nonuniform orientation of the AFM/FM exchange coupling is characteristic of different regions of the annealed film, which is perpendicular to the film plane in its regions containing hard-magnetic FM component, but it is oriented along the film plane in its parts with soft-magnetic properties as a result of strong pinning of their magnetic moments by IrMn layer in this direction.

An important effect of nonuniform magnetic ordering in the IrMn layer on the magnetoresistive properties of IrMn/[Co/Pd] films is revealed. It is found that MR of both continuous and porous films is mainly attributed to the electron-magnon scattering, with magnon magnetoresistance (MMR) being the dominant mechanism. However, the splitting of the porous film into the areas with different orientation of the AFM/FM exchange coupling allows partial rotation of magnetic moments of the near-interface parts of the IrMn layer. A pronounced unidirectional PMA in "AFM/hard-magnetic FM" structures combined with the in-plane anisotropy of the rest IrMn layer induces "unidirectional" MR effect in the porous film. Namely, a reduced resistance is formed in the external field oriented similarly to the unidirectional perpendicular anisotropy, while an increased resistance is detected in the opposite external field. The possibility of manipulating the orientation of magnetic moments in the AFM layer revealed in the porous IrMn/[Co/Pd] films opens the opportunity for their application in AFM spintronics.

ACCEPTED MANUSCRIPT
Journal of Applied Physics
AIP Publishing
This is the author's peer reviewed, accepted manuscript. However, the online version of record will be different from this version once it has been copyedited and typeset.
PLEASE CITE THIS ARTICLE AS DOI: 10.1063/5.0006194

AUTHORS CONTRIBUTION

All authors contributed equally to this work.

ACKNOWLEDGEMENTS

The authors acknowledge the financial support from the Vietnam Academy of Science and Technology under Projects QTBY01.04/19-20 and KHCTVL.03/19-20, the Belarusian State Research Program "Physical materials science, new materials and technologies" (task 2.44) and The Belarusian Republic Foundation for Fundamental Research (project no. F19V-005).

DATA AVAILABILITY STATEMENT

The data that supports the findings of this study are available from the corresponding author upon reasonable request.

REFERENCES

[1]D. N. H. Nam, W. Chen, K. G. West, D. M. Kirkwood, J. Lu, and S. A. Wolf, Appl. Phys. Letters 93, 152504 (2008). DOI: 10.1063/1.2999626

[2]S. Parkin, J. Xin, C. Kaiser, A. Panchula, K. Roche, and M.Samant, Proc. IEEE 91, 661 (2003). DOI: 10.1109/jproc.2003.811807

[3]B. Negulescu, D. Lacour, F. Montaigne, A. Gerken, J. Paul, V. Spetter, J. Marien, C. Duret, and M. Hehn, App. Phys. Letters. 95, 112502 (2009). DOI: 10.1063/1.3226676

[4]S. V. Dijken, J. Moritz, and J. M. D. Coey, J. Appl. Phys. 97, 063907 (2005). DOI: 10.1063/1.1861964

[5]W. H. Meiklejohn and C. P. Bean, Phys. Rev. 102, 1413 (1956).

[6]X. Martí, B. G. Park, J. Wunderlich, H. Reichlová, Y. Kurosaki, M. Yamada, H. Yamamoto, A. Nishide, J. Hayakawa, H. Takahashi, and T. Jungwirth, Phys. Rev. Letters 108, 017201 (2012). DOI: 10.1103/PhysRevLett.108.017201

[7]J.-V. Kim and R. L. Stamps, Phys. Rev. B 71, 094405 (2005). DOI: 10.1103/PhysRevB.71.094405

[8]A. P. Malozemoff, Phys. Rev. B 35, 3679 (1987).

[9]K. Takano, R. H. Kodama, A. E. Berkowitz, W. Cao, and G. Thomas, J. Appl. Phys. 83, 6888 (1998). DOI: 10.1063/1.367721

[10]W. Feng, N.-Y. Jiang, S.-D. Huang, H.-M. Chen, C.-W. Cheng, G. Chern, and C.-C. Yu, J. Appl. Phys. 111, 033904 (2012). DOI: 10.1063/1.3681174

ACCEPTED MANUSCRIPT
Journal of Applied Physics
AIP Publishing
This is the author's peer reviewed, accepted manuscript. However, the online version of record will be different from this version once it has been copyedited and typeset.
PLEASE CITE THIS ARTICLE AS DOI: 10.1063/5.0006194

[11]A. Scholl, M. Liberati, E. Arenholz, H. Ohldag, and J. Stöhr, Phys. Rev. Letters 92, 247201 (2004). DOI: 10.1103/PhysRevLett.92.247201

[12]B. G. Park, J. Wunderlich, X. Martí, V. Holý, Y. Kurosaki, M. Yamada, H. Yamamoto, A. Nishide, J. Hayakawa, H. Takahashi, A. B. Shick, and T. Jungwirth, Nature Materials 10, 347 (2011). DOI: 10.1038/NMAT2983

[13]J. Nogués and I. K. Schuller, J. Magn. Magn. Mater. 192, 203 (1999).

[14]J. Nogués, J. Sort, V. Langlais, V. Skumryev, S. Suriñach, J. S. Muñoz, and M.D. Baró, Phys. Rep. 422, 65 (2005). DOI: 10.1016/j.physrep.2005.08.004

[15]P. Kappenberger, S. Martin, Y. Pellmont, H. J. Hug, J. B. Kortright, O. Hellwig, and E. E. Fullerton, Phys. Rev. Letters 91, 267202 (2003). DOI: 10.1103/PhysRevLett.91.267202

[16]J. Sort, V. Baltz, F. Garcia, B. Rodmacq, and B. Dieny, Phys. Rev. B 71, 054411 (2005). DOI: 10.1103/PhysRevB.71.054411

[17]L. Lin, N. Thiyagarajah, H. W. Joo, J. Heo, K. A. Lee, and S. Bae, J. Appl. Phys. 108, 063924 (2010). DOI: 10.1063/1.3471803

[18]Q. Ying and L. Yifan, AIP Advances 8, 025314 (2018). DOI: 10.1063/1.5013159

[19]W.-B. Wu, J. Kasiuk, T. N. Anh Nguyen, J. Fedotova, J. Przewoźnik, C. Kapusta, O. Kupreeva, S. Lazarouk, K. T. Do, T. H. Nguyen, H. K. Vu, D. L. Vu, and J. Åkerman, Phys. Chem. Chem. Phys. 22, 3661 (2020). DOI: 10.1039/c9cp05947d

[20]H. Ohldag, A. Scholl, F. Nolting, S. Anders, F. U. Hillebrecht, and J. Stöhr, Phys. Rev. Letters 86, 2878 (2001). DOI: 10.1103/PhysRevLett.86.2878

[21]T. Jungwirth, X. Marti, P. Wadley, and J. Wunderlich, Nature Nanotechnology 11, 231 (2016). DOI: 10.1038/NNANO.2016.18

[22]V. Tshitoyan, C. Ciccarelli, A. P. Mihai, M. Ali, A. C. Irvine, T. A. Moore, T. Jungwirth, and A. J. Ferguson, Phys. Rev. B 92, 214406 (2015). DOI: 10.1103/PhysRevB.92.214406

[23]S. V. Dijken, M. Besnier, J. Moritz, and J. M. D. Coey, J. Appl. Phys. 97, 10K114 (2005). DOI: 10.1063/1.1855699

[24]G. Vinai, J. Moritz, S. Bandiera, I. L. Prejbeanu, and B. Dieny, J. Phys. D: Appl. Phys. 46, 322001 (2013). DOI: 10.1088/0022-3727/46/32/322001

[25]A. Kohn, A. Kovacs, R. Fan, G. J. McIntyre, R. C. Ward, and J. P. Goff, Sci. Rep. 3, 2412 (2013). DOI: 10.1038/srep02412

[26]M. Perzanowski, M. Marszalek, A. Zarzycki, M. Krupinski, A. Dziedzic, and Y. Zabila, ACS Appl. Mater. Interfaces 8, 28159 (2016). DOI: 10.1021/acsami.6b08532

ACCEPTED MANUSCRIPT
Journal of Applied Physics
AIP Publishing
This is the author's peer reviewed, accepted manuscript. However, the online version of record will be different from this version once it has been copyedited and typeset.
PLEASE CITE THIS ARTICLE AS DOI: 10.1063/5.0006194

[27]M. Tsunoda, K. Nishikawa, T. Damm, T. Hashimoto, and M. Takahashi, J. Magn. Magn. Mater. 239, 182 (2002). DOI: 10.1016/S0304-8853(01)00519-4

[28]J. Sort, F. Garcia, S. Auffret, B. Rodmacq, B. Dieny, V. Langlais, S. Suriñach, J. S. Muñoz, M. D. Baró, and J. Nogués, Appl. Phys. Letters 87, 242504 (2005). DOI: 10.1063/1.2139840

[29]X. T. Zhao, W. Liu, Z. M. Dai, D. Li, X. G. Zhao, Z. H. Wang, D. Kim, C. J. Choi, and Z. D. Zhang, Materials Letters 182, 185 (2016). DOI: 10.1016/j.matlet.2016.06.121

[30]M. Krupinski, D. Mitin, A. Zarzycki, A. Szkudlarek, M. Giersig, M. Albrecht, and M. Marszałek, Nanotechnology 28, 085302 (2017). DOI: 10.1088/1361-6528/aa5656

[31]M. T. Rahman, N. N. Shams, C. H. Lai, J. Fidler, and D. Suess, Phys. Rev. B 81, 014418 (2010). DOI: 10.1103/PhysRevB.81.014418

[32]M. T. Rahman, R. K. Dumas, N. Eibagi, N. N. Shams, Y.-C. Wu, K. Liu, and C.-H. Lai, Appl. Phys. Letters 94, 042507 (2009). DOI: 10.1063/1.3075061

[33]S. K. Lazarouk, D. A. Sasinovich, O. V. Kupreeva, T. I. Orehovskaia, N. Rochdi, F. Arnaud d'Avitaya, and V. E. Borisenko, Thin Solid Films, 526, 41 (2012).

[34]Y. F. Liu, J. W. Cai, and S. L. He, J. Phys. D: Appl. Phys. 42, 115002 (2009). DOI: 10.1088/0022-3727/42/11/115002

[35]T. N. Anh Nguyen, J. Fedotova, J. Kasiuk, V. Bayev, O. Kupreeva, S. Lazarouk, D. H. Manh, D. L. Vu, S. Chung, J. Åkerman, V. Altynov, and A. Maximenko. Appl. Surf. Sci. 427, 649 (2017). DOI: 10.1016/j.apsusc.2017.08.238

[36]J. Rodriguez-Carvajal, Physica B 192, 55 (1993). DOI: 10.1016/0921-4526(93)90108-I

[37]A. A. Jara, I. Barsukov, B. Youngblood, Y.-J. Chen, J. Read, H. Chen, P. Braganca, and I. N. Krivorotov, IEEE Magn. Letters 7, 3104805 (2016). DOI: 10.1109/LMAG.2016.2590464

[38]S.-K. Kim, Y.-M. Koo, A. C. Vladimir, J. B. Kortright, and S.-C. Shin, Phys. Rev. B. 62, 3025 (2000). DOI: 10.1103/PhysRevB.62.3025

[39]X. M. Liu, P. Ho, J. S. Chen, and A. O. Adeyeye, J. Appl. Phys. 112, 073902 (2012). DOI: 10.1063/1.4754858

[40]M. Heibel, G. Kumar, C. Wyse, P. Bukovec, and A. B. Bocarsly. Chem. Mater. 8, 1504 (1996). DOI: 10.1021/cm960105u

[41]H. W. King and F. D. Manchester, J. Phys. F: Metal Phys. 8, 15 (1978). DOI: 10.1088/0305-4608/8/1/007

[42]J.-H. Jang, C. Pak and Y.-U. Kwon, J. Power Sources 201, 179 (2012). DOI: 10.1016/j.jpowsour.2011.10.139

[43]C. Lindahl, H. Engqvist, and W. Xia, ISRN Biomater. 2013, 205601 (2013).

ACCEPTED MANUSCRIPT
Journal of Applied Physics
AIP Publishing
This is the author's peer reviewed, accepted manuscript. However, the online version of record will be different from this version once it has been copyedited and typeset.
PLEASE CITE THIS ARTICLE AS DOI: 10.1063/5.0006194

[44]J. Feng, H. F. Liu, H. X. Wei, X.-G. Zhang, Y. Ren, X. Li, Y. Wang, J. P. Wang, and X. F. Han, Phys. Rev. Appl. 7, 054005 (2017). DOI: 10.1103/PhysRevApplied.7.054005

[45]T. N. Anh Nguyen, J. Fedotova, J. Kasiuk, W. B. Wu, J. Przewoźnik, C. Kapusta, O. Kupreeva, S. Lazarouk, T. H. T. Trinh, K. T. Du, H. M. Du, D. L. Vu, and J. Åkerman, J. Electronic Materials 48, 1492 (2019). DOI: 10.1007/s11664-018-06847-3

[46]A. van den Brink, G. Vermijs, A. Solignac, J. Koo, J. T. Kohlhepp, H. J. M. Swagten, and B. Koopmans, Nature Communications 7,10854 (2016). DOI: 10.1038/ncomms10854

[47]Y.Y. Wang, C. Song, B. Cui, G.Y. Wang, F. Zeng, and F. Pan, Phys. Rev. Letters 109, 137201 (2012). DOI: 10.1103/PhysRevLett.109.137201

[48]J. V. Kasiuk, A. A. Maksimenko, J. A. Fedotova, M. Marszałek, S. K. Lazaruk, and O. V. Kupreeva, Physics of the Solid State 58, 2312 (2016). DOI: 10.1134/S1063783416110160

[49]M. Perzanowski, M. Krupinski, A. Zarzycki, A. Dziedzic, Y. Zabila, and M. Marszalek, ACS Appl. Mater. Interfaces 9, 33250 (2017). DOI: 10.1021/acsami.7b07665

[50]D. Wu, Z. Zhang, L. Li, Z. Zhang, H. B. Zhao, J. Wang, B. Ma, and Q. Y. Jin, Sci. Rep. 5, 12352 (2015). DOI: 10.1038/srep12352

[51]C. A. F. Vaz, J. A. C. Bland, and G. Lauhoff, Reports on Progress in Physics 71, 056501 (2008). DOI: 10.1088/0034-4885/71/5/056501

[52]K. Saravanan, C.-H. Kao, Y.-C. Shao, Y.-F. Wang, B.-Y. Wang, H. T. Wang, C.-J. Tsai, W.-C. Lin, C.-W. Pao, H.-M. Tsai, L.-Y. Jang, H. J. Lin, J.-F. Lee, and W.-F. Pong, RSC Advances 5, 19014 (2015). DOI: 10.1039/c4ra15683h

[53]M. Stark, F. Schlickeiser, D. Nissen, B. Hebler, P. Graus, D. Hinzke, E. Scheer, P. Leiderer, M. Fonin, M. Albrecht, U. Nowak, and J. Boneberg, Nanotechnology 26, 205302 (2015). DOI: 10.1088/0957-4484/26/20/205302

[54]B. Raquet, M. Viret, E. Sondergard, O. Cespedes, and R. Mamy, Phys. Rev. B 66, 024433 (2002). DOI: 10.1103/PhysRevB.66.024433

[55]A. P. Mihai, J. P. Attané, A. Marty, P. Warin, and Y. Samson, Phys. Rev. B 77, 060401 (2008). DOI: 10.1103/PhysRevB.77.060401

[56]X. Ji, A. B. Pakhomov, and K. M. Krishnan, J. Appl. Phys. 101, 09E507 (2007); DOI: 10.1063/1.2710227

[57]D. Ravelosona, A. Cebollada, F. Briones, C. Diaz-Paniagua, M. A. Hidalgo, F. Batallan, Phys. Rev. B 59, 4322 (1999). DOI: 10.1103/PhysRevB.59.4322

AIP Publishing

Journal of Applied Physics

ACCEPTED MANUSCRIPT

This is the author's peer reviewed, accepted manuscript. However, the online version of record will be different from this version once it has been copyedited and typeset.

PLEASE CITE THIS ARTICLE AS DOI: 10.1063/5.0006194

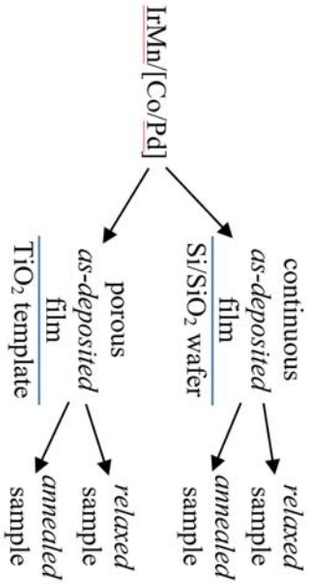

AIP Publishing

Journal of Applied Physics

ACCEPTED MANUSCRIPT

This is the author's peer reviewed, accepted manuscript. However, the online version of record will be different from this version once it has been copyedited and typeset.

PLEASE CITE THIS ARTICLE AS DOI: 10.1063/5.0006194

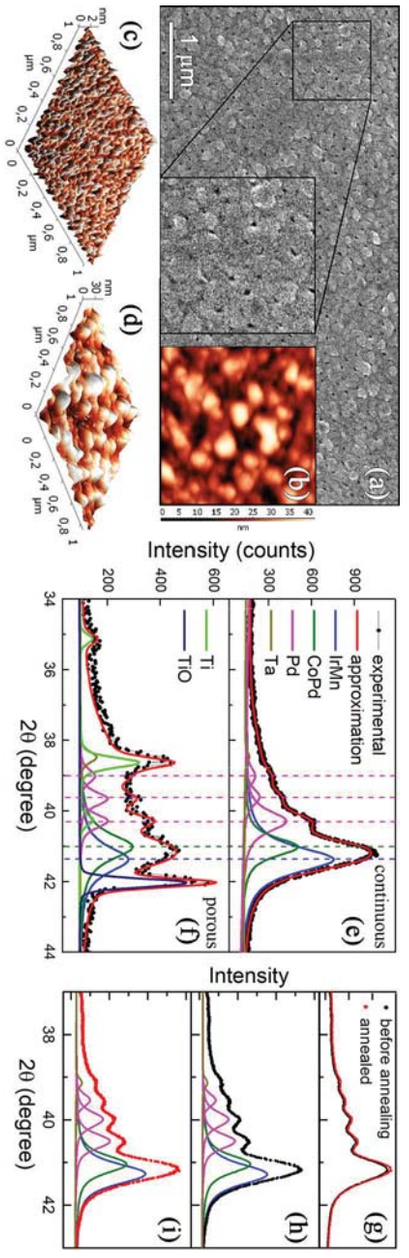

ACCEPTED MANUSCRIPT

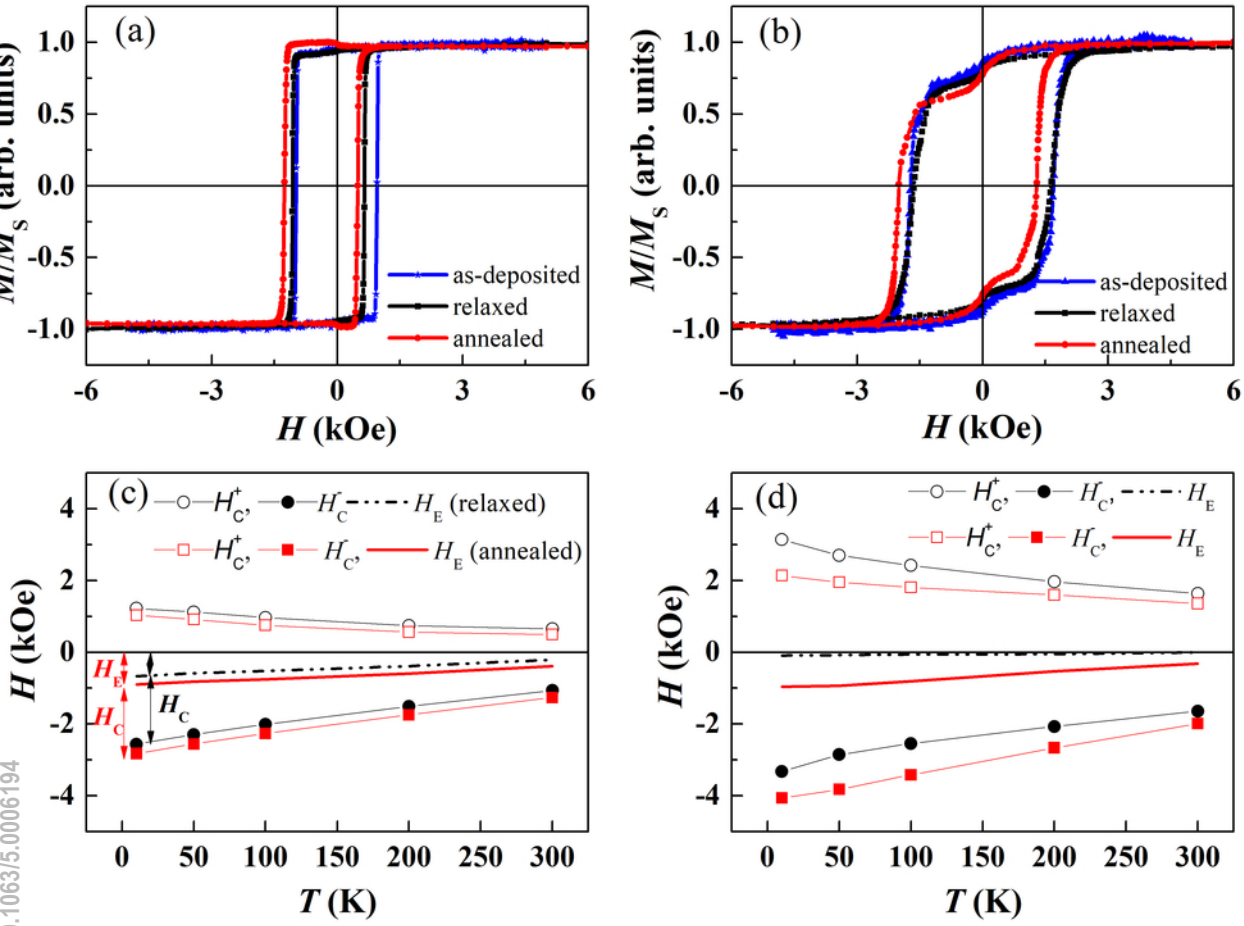

This is the author's peer reviewed, accepted manuscript. However, the online version of record will be different from this version once it has been copyedited and typeset.
PLEASE CITE THIS ARTICLE AS DOI: 10.1063/5.0006194

Journal of Applied Physics

AIP Publishing

AIP Publishing

Journal of Applied Physics

ACCEPTED MANUSCRIPT

This is the author's peer reviewed, accepted manuscript. However, the online version of record will be different from this version once it has been copyedited and typeset.
PLEASE CITE THIS ARTICLE AS DOI: 10.1063/5.0006194

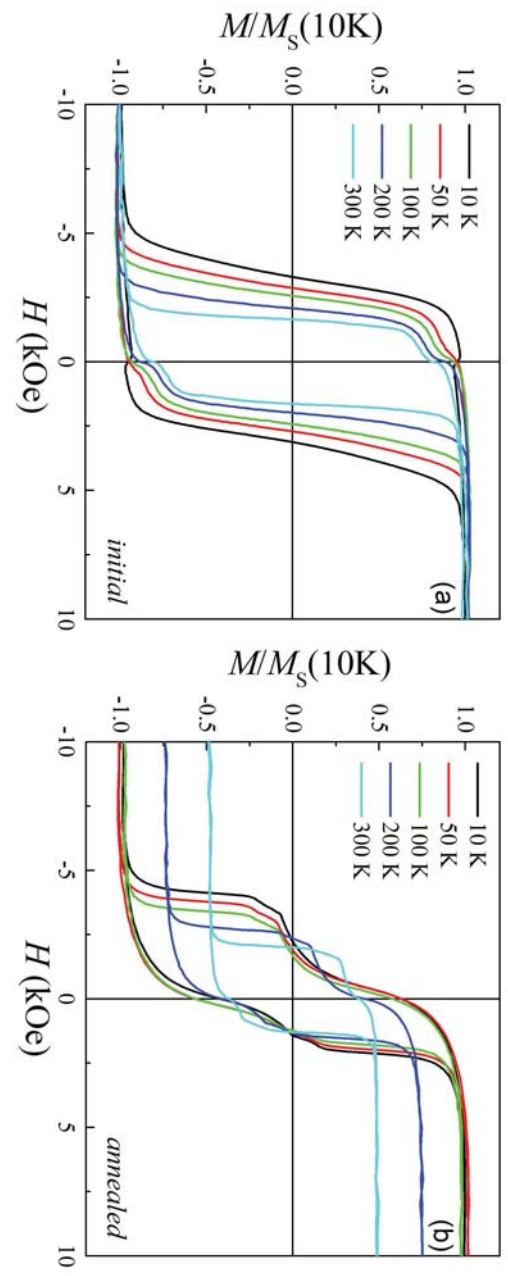

AIP Publishing

Journal of Applied Physics

ACCEPTED MANUSCRIPT

This is the author's peer reviewed, accepted manuscript. However, the online version of record will be different from this version once it has been copyedited and typeset.
PLEASE CITE THIS ARTICLE AS DOI: 10.1063/5.0006194

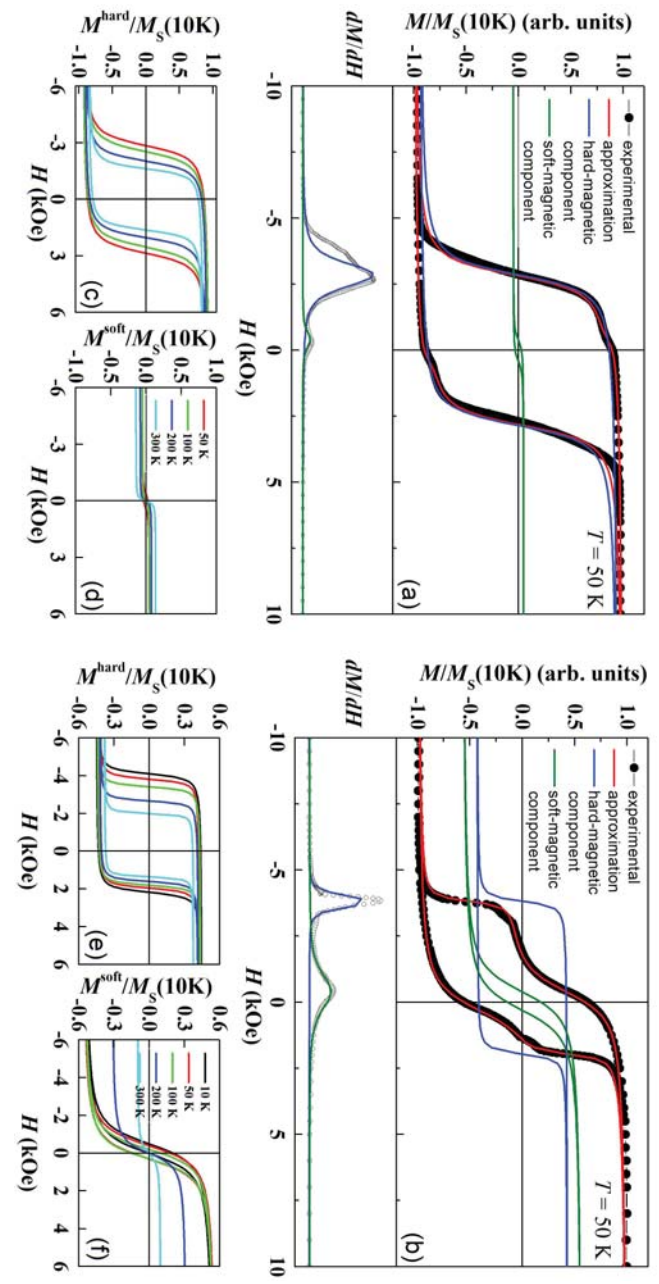

AIP Publishing

Journal of Applied Physics

ACCEPTED MANUSCRIPT

This is the author's peer reviewed, accepted manuscript. However, the online version of record will be different from this version once it has been copyedited and typeset.
PLEASE CITE THIS ARTICLE AS DOI: 10.1063/5.0006194

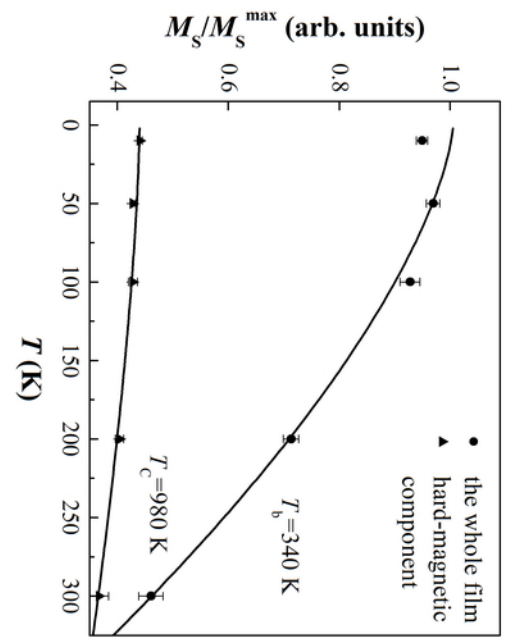

AIP Publishing
Journal of Applied Physics

ACCEPTED MANUSCRIPT

This is the author's peer reviewed, accepted manuscript. However, the online version of record will be different from this version once it has been copyedited and typeset.

PLEASE CITE THIS ARTICLE AS DOI: 10.1063/5.0006194

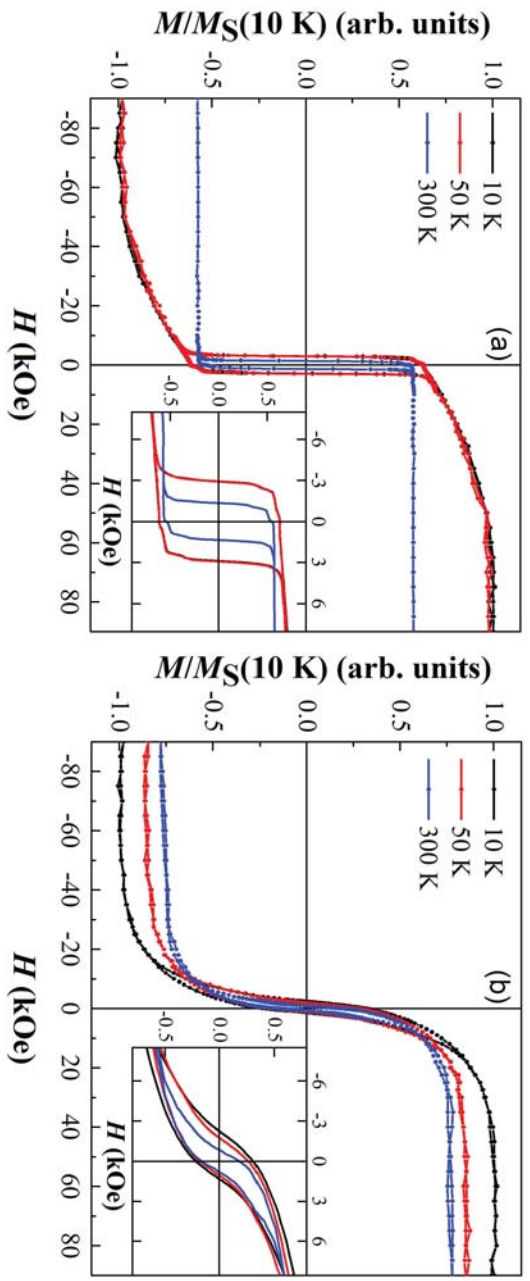

AIP Publishing

Journal of Applied Physics

ACCEPTED MANUSCRIPT

This is the author's peer reviewed, accepted manuscript. However, the online version of record will be different from this version once it has been copyedited and typeset.
PLEASE CITE THIS ARTICLE AS DOI: 10.1063/5.0006194

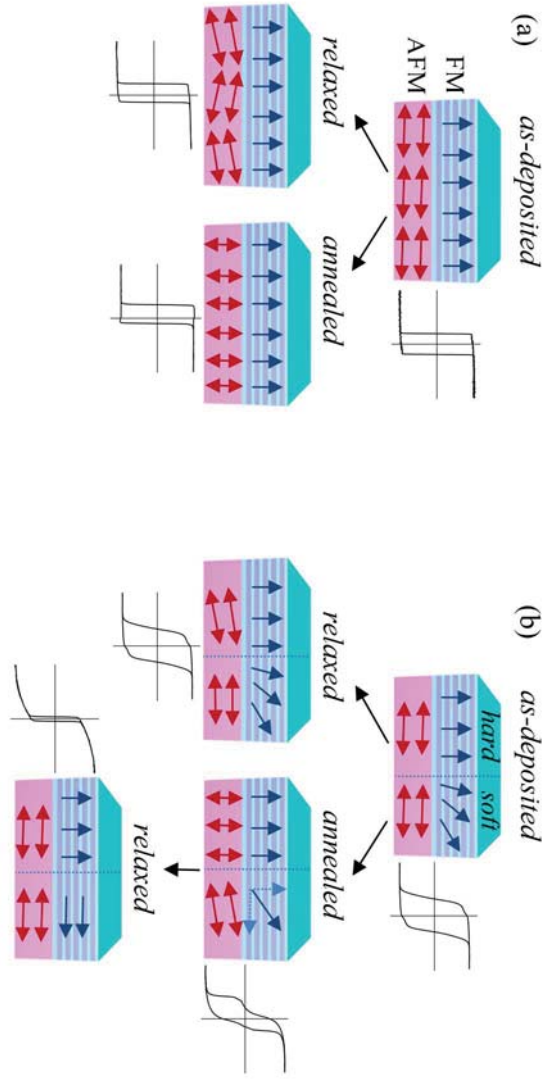

AIP Publishing

Journal of Applied Physics

ACCEPTED MANUSCRIPT

This is the author's peer reviewed, accepted manuscript. However, the online version of record will be different from this version once it has been copyedited and typeset.

PLEASE CITE THIS ARTICLE AS DOI: 10.1063/5.0006154

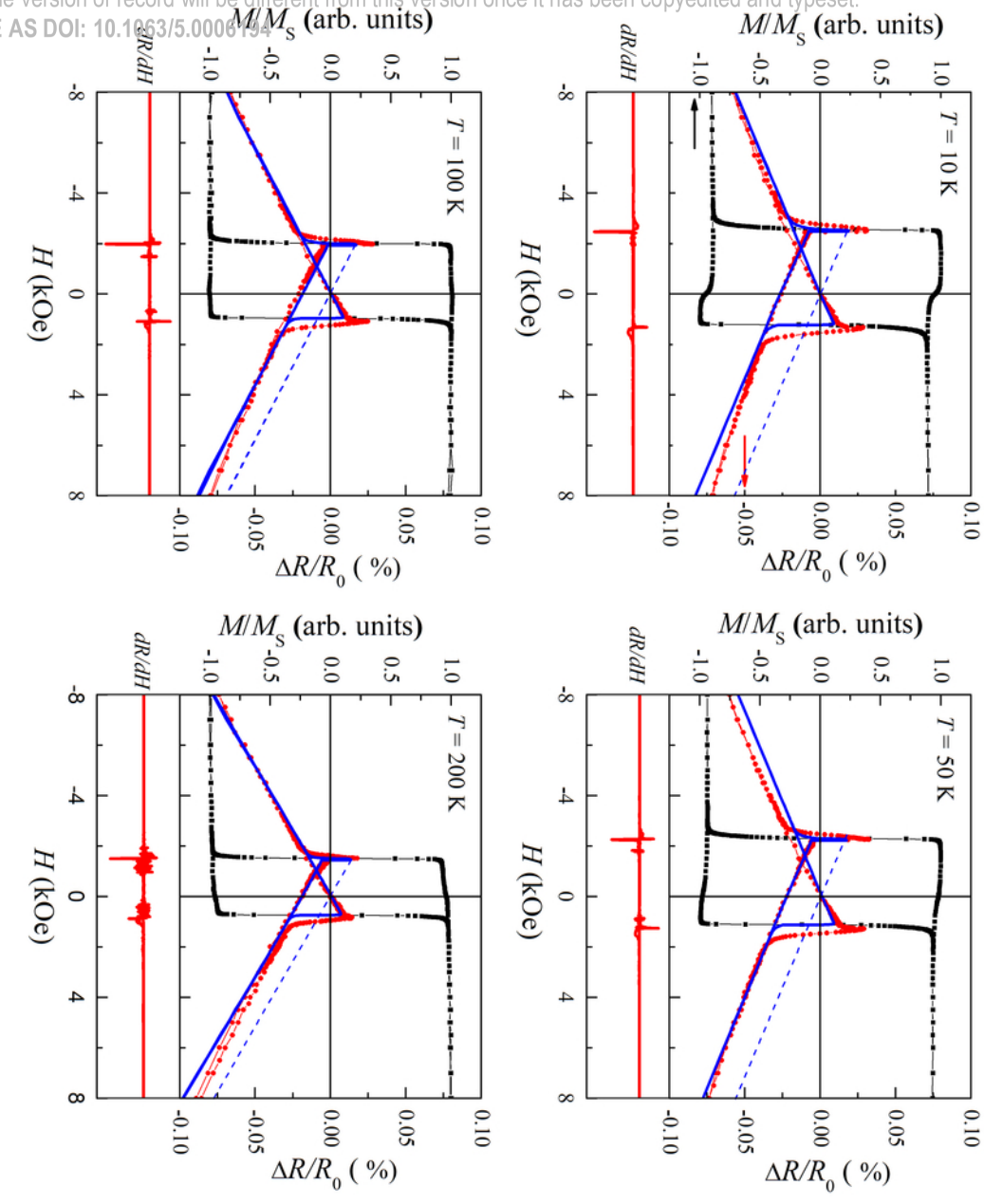

View publication stats

AIP Publishing

Journal of Applied Physics

ACCEPTED MANUSCRIPT

This is the author's peer reviewed, accepted manuscript. However, the online version of record will be different from this version once it has been copyedited and typeset.

PLEASE CITE THIS ARTICLE AS DOI: 10.1063/5.0006154